

Cubic Phase Function: A Simple Solution to Polynomial Phase Signal Analysis

Djurovic, Igor; Simeunovic, Marko; Wang, Pu

TR2017-019 June 01, 2017

Abstract

This article provides an overview of the cubic phase function (CPF) as a tool proposed for both parametric and nonparametric estimation of the frequency modulated (FM) and in particular polynomial phase signals (PPS). This simple tool motivated small revolution in this field with numerous extensions and applications. We are describing the CPF and compare some of its extensions for both one-dimensional and twodimensional signals. The comparisons are performed in terms of accuracy (measured with signal-to-noise (SNR) threshold and mean-squared error (MSE)) and computational complexity. Also, we review the CPF and related transforms applications.

Signal Processing (Elsevier)

© 2017 MERL. This work may not be copied or reproduced in whole or in part for any commercial purpose. Permission to copy in whole or in part without payment of fee is granted for nonprofit educational and research purposes provided that all such whole or partial copies include the following: a notice that such copying is by permission of Mitsubishi Electric Research Laboratories, Inc.; an acknowledgment of the authors and individual contributions to the work; and all applicable portions of the copyright notice. Copying, reproduction, or republishing for any other purpose shall require a license with payment of fee to Mitsubishi Electric Research Laboratories, Inc. All rights reserved.

Cubic Phase Function: A Simple Solution to Polynomial Phase Signal Analysis

Igor Djurović, Marko Simeunović and Pu Wang

Abstract— This article provides an overview of the cubic phase function (CPF) as a tool proposed for both parametric and nonparametric estimation of the frequency modulated (FM) and in particular polynomial phase signals (PPS). This simple tool motivated small revolution in this field with numerous extensions and applications. We are describing the CPF and compare some of its extensions for both one-dimensional and two-dimensional signals. The comparisons are performed in terms of accuracy (measured with signal-to-noise (SNR) threshold and mean-squared error (MSE)) and computational complexity. Also, we review the CPF and related transforms applications.

Keywords: Frequency modulated signals, time-frequency analysis, polynomial phase signals, parameter estimation, cubic phase function, chirp-rate, instantaneous frequency.

I. INTRODUCTION

Engineers in many fields often encounter non-stationary signals including biological, speech and music signals, radio signals in wireless communications and radars, and dispersive seismic signals [1]– [57]. The conventional Fourier transform (FT), a popular tool to bridge between time and frequency, is considered to be inadequate to analyze such real-life signals [1], [2], [4]. In contrast, joint time-frequency (TF) analysis is an efficient way to reveal frequency contents of signals evolving over time, alternatively known as the instantaneous frequency (IF).

One particularly interesting model of non-stationary signals is the polynomial phase signal (PPS) model. The last 25 years have witnessed tremendous developments in the area of PPS parameter estimation, driven by applications originated in radars, sonars, biomedicine, machine engine testing, etc. [58]– [95]. The maximum likelihood (ML) estimator has limited application due to a required multi-dimensional search over the parameter space. Early developments for the PPS parameter estimation are based on high-order ambiguity function (HAF) and its product form (PHAF) [91], [96]. The HAF-based estimation procedure consists of phase order decrementing by the process known as the phase differentiation (PD) until obtained signal is a sinusoid (the PPS of the first order).

I. Djurović is with the Electrical Engineering Department, University of Montenegro, Cetinjski put bb, 81 000 Podgorica, Montenegro. He is also with the Institute for Cutting Edge Information and Communication Technologies, Džordža Vašingtona 66/354, Podgorica, Montenegro (e-mail: igordj@ac.me).

M. Simeunović is with the Faculty for Information Systems and Technologies, University of Donja Gorica, Oktoih 1, 81 000 Podgorica, Montenegro. He is also with the Institute for Cutting Edge Information and Communication Technologies, Džordža Vašingtona 66/354, Podgorica, Montenegro (e-mail: markos@ac.me).

P. Wang is with Mitsubishi Electric Research Laboratories (MERL), 201 Broadway, Cambridge, MA 02139, USA (e-mail: pwang@merl.com).

Then, the highest-order phase parameter is estimated using the fast algorithm, i.e., by an one-dimensional (1-D) search over the parameter space. This strategy is efficient but with numerous shortcomings. Firstly, in each stage of the procedure, the PD (performed by the auto-correlation function) reduces signal length and increases the number of noise-related terms in the resulted signal. These effects increase the signal-to-noise-ratio (SNR) threshold and estimation mean squared error (MSE). The auto-correlation also introduces cross-terms when multicomponent signals are considered. Finally, after estimation of the highest-order phase parameter, the same procedure is performed on the dechirped signal. Dechirping procedure causes error propagation from higher- to lower-order phase parameters. Some negative effects of the HAF, in particular cross-terms, are mitigated using the PHAF obtained as the multiplication of several HAFs calculated with different lag sets sharing the same product. The alternative technique is the integrated generalized ambiguity function (IGAF) [97]. It is accurate but, unfortunately, with heavy computations. Specifically this technique requires integrations over multi-dimensional lag space. Large number of integrals (or sums), i.e., calculation complexity, limits application of the IGAF to lower-order PPSs. Nevertheless, the IGAF is known to enhance the signal term and suppress the oscillating cross-terms and noise from the (coherent) lag integrations. In addition, two highest-order parameters are estimated at once meaning that the effect of error propagation is also reduced.

Aside from the IF, instantaneous frequency rate (IFR) or chirp-rate (CR) provides additional insights into the signal's frequency changing rate [1], [2], [98]–[100] and has received significant attention after O'Shea's seminal paper of [88]. At first, O'Shea proposed the original cubic phase function (CPF) for the parameter estimation of a third-order PPS, i.e., a cubic phase (CP) signal [88], [89]. The CPF-based procedure requires only one PD resulting in significantly better performances with respect to the (P)HAF-based alternatives for the CP signal. Later, numerous researchers strive for its extensions to higher-order PPSs [69], [70], [101]– [104]. Besides, the CPF maps a signal to a 2-D joint time-chirp (frequency) rate domain. The time-CR domain and representations are still not well understood compared to the TF domain and representations. Meanwhile, there exist considerable interests in generalization of this transform to a 2-D PPS [67].

The aim of this paper is to show how this, at the first glance, simple modification of the CPF can motivate significant developments in the field of the PPS estimation and in more general nonstationary signal analysis. These developments resulted in significant improvement in the PPS estimation performance

with respect to the state-of-the-art techniques. This overview article is devoted to the CPF since this transform and related approaches still reverberate in the community working with both theoretical and practical developments in the PPS estimation and with general nonstationary phase signals. The remaining of this paper is organized as follows. Theoretical background on the CPF is given in Section II with basic performance analysis of this technique both in parametric and nonparametric estimation. Various extensions of the CPF are presented and compared in Section III. 2-D PPSs are considered in Section IV, while Section V brings literature overview of some practical applications where the CPF is used or where CP signals appear.

II. THEORETICAL OVERVIEW

A. Signal model

Consider a frequency modulated (FM) signal

$$x(t) = A \exp(j\phi(t)), \quad (1)$$

where A is the amplitude, and $\phi(t)$ is the signal phase. The first derivative of $\phi(t)$ is defined as the IF, $\omega(t) = \phi'(t)$, while its the second derivative is commonly referred to as the CR (or IFR) $\Omega(t) = \phi''(t)$. Assume that the observed signal $x(t)$ is corrupted by the complex zero-mean white Gaussian noise $\nu(t)$ with variance σ^2

$$y(t) = x(t) + \nu(t). \quad (2)$$

The discrete version of signal (2) is obtained by sampling $y(t)$ with a sampling interval Δt : $y(n) = y(n\Delta t) = x(n\Delta t) + \nu(n\Delta t)$, with N denoting the number of discrete samples. One of the most commonly considered parametric models of the FM signals is the PPS:

$$x(n) = A \exp(j\phi(n)) = A \exp\left(j \sum_{i=0}^P a_i n^i\right), \quad (3)$$

where a_i is the i th polynomial phase coefficient and P is the PPS order.

For nonparametric estimators, i.e., no parametric form of $\phi(t)$ is assumed, the goal is to estimate the IF ($\omega(n)$) or the CR ($\Omega(n)$) from noisy observations $y(n)$ for all n , while parametric estimators obtain signal parameters $\{A; a_i, i = 0, \dots, P\}$ by relying on some parametric form of $\phi(n)$, for instance, the polynomial phase form in (3). Parameters a_i , $i = 0, \dots, P$ are called phase parameters and a_P is known as the highest-order phase parameter.

Two performance measures of parametric estimators are the accuracy and computational complexity. The computational complexity is the number of algorithmic operations represented in the big-O notation $O(\cdot)$ [106]. The estimation accuracy is measured with two metrics: the MSE and SNR threshold. Specifically, the MSE can be numerically computed as

$$\text{MSE}\{\hat{a}\} = \frac{1}{N_{\text{trial}}} \sum_{k=1}^{N_{\text{trial}}} (a - \hat{a}_k)^2, \quad (4)$$

where \hat{a}_k is parameter estimate in the k th trial while N_{trial} is the number of Monte-Carlo runs. The SNR threshold is

an SNR value below which the numerical performance is significantly deviated from the expected theoretically derived performance [107]. Albeit of other definitions of the SNR threshold of the estimation procedure we will perform simple visual inspection based on the MSE rapid departure from the Cramer-Rao lower bound (CRLB).

B. The maximum likelihood estimator

The ML estimation procedure can be described as (we assume P is known)

$$(\hat{a}_1, \dots, \hat{a}_P) = \arg \max_{(b_1, \dots, b_P)} \text{ML}(b_1, b_2, \dots, b_P) \quad (5)$$

$$\text{ML}(b_1, b_2, \dots, b_P) = \left| \sum_n y(n) \exp\left(-j \sum_{i=1}^P b_i n^i\right) \right|^2 \quad (6)$$

Then, the amplitude A and initial phase a_0 can be estimated as

$$\hat{A} = \frac{1}{N} \sum_n |y_d(n)| \quad (7)$$

$$\hat{a}_0 = \frac{1}{N} \sum_n \angle y_d(n), \quad (8)$$

using the dechirped signal $y_d(n) = y(n) \exp\left(-j \sum_{i=1}^P \hat{a}_i n^i\right)$. The ML estimation needs to perform a P -dimensional search $O(N^P)$ over the P -dimensional parameter space (b_1, b_2, \dots, b_P) . For $P > 3$, the direct search is computationally prohibitive.

To avoid the multi-dimensional search, suboptimal techniques are proposed with reduction of the search space. This reduced search space is formed by successively decrementing the polynomial order in the signal phase by the PD process as described in Section II-D.

C. Cramér-Rao lower bound

The best achievable performance bound of all unbiased parametric PPS estimators is the CRLB. It is derived in [108], [109], and for general PPS it exhibits:

$$\text{CRLB}\{\hat{a}_i\} = \frac{\sigma^2}{2A^2} (\mathbf{D}_{P+1}^{-1} \mathbf{H}_{P+1}^{-1} \mathbf{D}_{P+1}^{-1})_{i,i} \quad (9)$$

where the (k, l) th element of $(P+1) \times (P+1)$ matrix \mathbf{H}_{P+1} is $\sum_n n^{k+l}$ while the matrix \mathbf{D}_{P+1} is a diagonal matrix with elements $(\Delta t)^i$, $i \in [0, P]$. Here, the exponent -1 denotes the matrix inverse while index i, i corresponds to the (i, i) element of the resulting matrix. In general, the CRLB for phase parameters a_i can be simplified as

$$\text{CRLB}\{\hat{a}_i\} = \alpha_{iP} \frac{\sigma^2}{A^2 N^{2P+1} (\Delta t)^{2P}}, \quad (10)$$

where α_{iP} is a constant scalar dependent on i and P .

D. HAF/PHAF estimator

Instead of the P -dimensional search of the ML estimation, an alternative solution is to successively reduce the PPS order, ideally to a single-tone sinusoid, and estimate the phase information from the reduced-order PPS. The phase order can be reduced using the PD recursively defined as:

$$\text{PD}^1[n, \tau_1] = r_{yy}(n, \tau_1) = y(n + \tau_1)y^*(n - \tau_1), \quad (11)$$

$$\begin{aligned} \text{PD}^Q[n; \tau_1, \dots, \tau_Q] &= \text{PD}^{Q-1}[n + \tau_Q; \tau_1, \dots, \tau_{Q-1}] \\ &\times \{ \text{PD}^{Q-1}[n - \tau_Q; \tau_1, \dots, \tau_{Q-1}] \}^*, \quad Q > 1 \end{aligned} \quad (12)$$

where τ_i , $i = 1, 2, \dots, Q$ are lag parameters and Q is the PD order. In each stage, the PD operator reduces the PPS order by one. Therefore, the resulting $\text{PD}^{P-1}[n; \tau_1, \tau_2, \dots, \tau_{P-1}]$ is a complex sinusoidal with frequency proportional to the highest-order phase parameter, $\omega = 2^{P-1}P!a_P \prod_{i=1}^{P-1} \tau_i$. For example if the third-order PPS is considered $P = 3$, i.e., the CP signal

$$x(n) = Ae^{j \sum_{i=0}^3 a_i n^i} = Ae^{ja_3 n^3 + ja_2 n^2 + ja_1 n + ja_0}, \quad (13)$$

the first PD:

$$\begin{aligned} \text{PD}^1[n, \tau_1] &= r_{xx}(n, \tau_1) \\ &= |A|^2 e^{j6a_3 \tau_1 n^2 + j4a_2 \tau_1 n + j(2a_3 \tau_1^3 + j2a_1 \tau_1)} \end{aligned} \quad (14)$$

represents the second-order PPS with parameters $b_2 = 6a_3 \tau_1$, $b_1 = 4a_2 \tau_1$ and $b_0 = 2a_3 \tau_1^3 + j2a_1 \tau_1$. The next PD equals to

$$\text{PD}^2[n; \tau_1, \tau_1] = |A|^4 \exp(j24a_3 \tau_1 \tau_2 n + j8a_2 \tau_1 \tau_2). \quad (15)$$

For a noise-free signal $\text{PD}^2[n; \tau_1, \tau_1]$ is a complex sinusoidal with the amplitude $|A|^4$, frequency $24a_3 \tau_1 \tau_2$, and initial phase $8a_2 \tau_1 \tau_2$.

The parameter a_P can be estimated by the high-order ambiguity function (HAF) using the following procedure:

$$\text{HAF}[\omega; \tau_1, \dots, \tau_{P-1}] = \sum_n \text{PD}^{P-1}[n, \tau_1, \dots, \tau_{P-1}] e^{-j\omega n}, \quad (16)$$

$$\hat{a}_P = \frac{1}{2^{P-1}P! \prod_{i=1}^{P-1} \tau_i} \arg \max_{\omega} |\text{HAF}(\omega; \tau_1, \dots, \tau_{P-1})|^2. \quad (17)$$

The effective number of samples in the HAF or $\text{PD}^{P-1}[n, \tau_1, \dots, \tau_{P-1}]$ is less than the number of raw samples N . Once a_P is estimated, the lower-order phase coefficients can be estimated from the dechirped signal $\tilde{y}(n) = y(n) \exp(-j\hat{a}_P n^P)$ using the similar procedure.

The described technique has several issues. Firstly, the auto-correlation operation in (11) and (12) shortens the signal and amplifies the noise. The second issue is the error propagation from estimated the highest-order parameters toward lower-order ones since $\tilde{y}(n)$ consists of some uncompensated part related to error $\Delta a_P = a_P - \hat{a}_P$. Since the HAF is obtained using the FT, frequency of $\text{PD}^{P-1}[n, \tau_1, \dots, \tau_{P-1}]$ should satisfy the sampling theorem, i.e., $|2^{P-1}P! \prod_{i=1}^{P-1} \tau_i a_P| < \pi$. Otherwise, the identifiability problem appears. More details on this issue can be found in [110], [111]. Finally, cross-terms occur for the multicomponent PPSs: $y(n) = \sum_{j=1}^M x_j(n) + \nu(n)$ where $x_j(n)$, $j = 1, \dots, M$, are PPSs. The first auto-correlation (11) (first-order PD) would have $M(M-1)/2 - M$

cross-terms with number rapidly increasing for next phase differentiation required for high-order PPSs.

One of potential strategies for solving the last problem is evaluation of the PDs with various lag sets:

$$\text{PD}^{P-1}[n, \tau_1^{(l)}, \dots, \tau_{P-1}^{(l)}], \quad l = 1, \dots, L. \quad (18)$$

Then, the HAF is evaluated for each lag set:

$$\text{HAF}[\omega; \tau_1^{(l)}, \dots, \tau_{P-1}^{(l)}] = \sum_n \text{PD}^{P-1}[n, \tau_1^{(l)}, \dots, \tau_{P-1}^{(l)}] e^{-j\omega F_l n}, \quad (19)$$

where $l = 1, \dots, L$ and $F_l = \prod_{i=1}^{P-1} \tau_i^{(l)} / \prod_{i=1}^{P-1} \tau_i^{(1)}$ is the frequency scaling factor. The PHAF is obtained as the product of L HAFs

$$\text{PHAF}(\omega) = \prod_{l=1}^L \text{HAF}[\omega; \tau_1^{(l)}, \dots, \tau_{P-1}^{(l)}] \quad (20)$$

and the highest-order parameter is estimated by using:

$$\hat{a}_P = \frac{1}{2^{P-1}P! \prod_{i=1}^{P-1} \tau_i^{(l)}} \arg \max_{\omega} |\text{PHAF}(\omega)|. \quad (21)$$

The selection of lag sets in the HAF and PHAF has been addressed in [94] and [96]. It has been shown that the lowest MSE in the HAF is achieved for $\tau^{\text{opt}} = \tau_1 = \tau_2 = \dots = \tau_{P-1} = N/(2P)$. In the case of the PHAF only one of lag sets can be selected in such manner. The other lag sets have to differ at least slightly from these values. A common practice is to keep the product of lag coefficients $\prod_{i=1}^{P-1} \tau_i^{(l)}$ as a constant in order to avoid interpolation.

If the lag sets are selected properly, the cross-terms caused by multiple signal components will be dislocated in various HAFs, $\text{HAF}[\omega; \tau_1^{(l)}, \dots, \tau_{P-1}^{(l)}]$, while all auto-terms will be concentrated at the same frequency. Therefore, the cross-terms are significantly attenuated by the product operation due to the misalignment at the frequency, while the auto-terms are coherently multiplied at the same frequency. The PHAF is well suited for multicomponent signal case but it has room for improvements related to the noise influence. Details related to multicomponent signal handling are available in Section III-H.

There are still remaining issues on the PHAF. For example, for the high-order PPS where several auto-correlations are required, the number of interference terms in the HAFs for the multicomponent signal can be large and it is impossible for distinguishing useful components from such a mixture. Performance in noise of the PHAF is slightly better than of the HAF. For a long time these two approaches were state-of-the-art in this field and it was assumed that they have reached the best achievable results with reasonable calculation complexity. However, the CPF introduced in [88] has shown that there is huge potential room for improvement of the PPS estimators.

To conclude, the main advantage of the (P)HAF approach remains calculation complexity that is of the order $O(PN \log_2 N)$.

E. Time-frequency representations

The TF representations are tools mapping the time-domain signal to the 2-D TF domain [4], [58], [59]. They are designed to be concentrated around the IF [1], [2], [112]. For example,

the Wigner distribution (WD) in the windowed (pseudo) discrete-time form is given as:

$$\begin{aligned} \text{WD}(t, \omega) &= \sum_n w(n)y(t+n)y^*(t-n) \exp(-j2\omega n) \\ &= \sum_n w(n)r_{yy}(t, n) \exp(-j2\omega n), \end{aligned} \quad (22)$$

where $w(n)$ is the window function. For the linear FM signal, $x(t) = A \exp(jat^2/2 + jbt + jc)$, the WD is ideally concentrated on the IF, $\omega(t) = at + b$,

$$\text{WD}(t, \omega) = 2\pi W(\omega - at - b), \quad (23)$$

where $W(\omega)$ is the FT of the window function. The IF can be estimated from peaks of the WD as [1]- [3], [36], [112], [113]:

$$\hat{\omega}(t) = \arg \max_{\omega} \text{WD}(t, \omega). \quad (24)$$

For other nonlinear modulations, the WD is not concentrated on the IF, but close to the IF. Note that the phase of the local auto-correlation $r_{yy}(t, n)$ using the modified Taylor's series expansion can be written as [114], [115], [116]:

$$\begin{aligned} \Phi(t, n) &= \phi(t+n) - \phi(t-n) \\ &\approx 2\phi'(t)n + \phi'''(t)\frac{n^3}{3} + \phi^{(5)}(t)\frac{n^5}{60} + \dots \end{aligned} \quad (25)$$

where $\phi^{(a)}(t)$ denotes the a th derivative of the signal phase. If higher-order phase terms are equal to 0, i.e., $\phi^{(a)}(t) = 0$ for $a > 2$, the WD is concentrated on the IF. As a result, a well-known central phase difference approximation follows:

$$\phi'(t) \approx \frac{\phi(t+n) - \phi(t-n)}{2n}. \quad (26)$$

Therefore, we can now establish a simple link between the difference formula and the TF representation. The positive term in the denominator corresponds to the signal with the same argument ($\phi(t+n) \rightarrow y(t+n)$), while the negative term corresponds to the conjugate term ($-\phi(t-n) \rightarrow y^*(t-n)$). Argument of the complex exponential is quantity of interest (in this case the IF ω) multiplied with the denominator of (26) ($\exp(-j2\omega n)$).

F. Cubic phase function

Estimation of the higher-order phase terms is also important [62], [92], [96], [97], [117], and in general, it requires higher-order non-linearity estimators that cause degradation of estimation performance with respect to additive noise.

To estimate the second-order phase derivative, i.e. the CR, consider the following finite difference equation

$$\phi''(t) \approx \frac{\phi(t+n) - 2\phi(t) + \phi(t-n)}{n^2}. \quad (27)$$

Signal $z(t; n) = y(t+n)y^{*2}(t)y(t-n)$ has the phase term that corresponds to $\phi''(t)$. It can be noticed that term caused by $y^{*2}(t)$ does not depend on n neither does the magnitude

of the local auto-correlation function. Therefore, the second-order phase derivative (CR) can be estimated by using the auto-correlation function $r_{yy}(t, n) = y(t+n)y(t-n)$ as [88]:

$$\begin{aligned} C(t, \Omega) &= \sum_n w(n)y(t+n)y(t-n) \exp(-j\Omega n^2) \\ &= \sum_n w(n)r_{yy}(t, n) \exp(-j\Omega n^2), \end{aligned} \quad (28) \quad (29)$$

where $C(t, \Omega)$ is referred as the CPF, and Ω denotes the CR index. Estimation of the CR then can be performed as:

$$\hat{\Omega}(t) = \arg \max_{\Omega} |C(t, \Omega)|. \quad (30)$$

In this way, the second-order phase derivative is estimated using the same order of nonlinearity as the first derivative, i.e., IF, in the WD. However, unlike the WD, the CPF is not real-valued as the WD. Many other properties from the TF representations are different in the generic time-CR domain (some of them are listed at the end of this section) making challenging application of numerous well developed tricks from the TF analysis to this domain.

In the rest of this section we are going to present findings related to the CPF application to the PPS estimation problems of CP signals. Then, we will discuss its application to the CR estimation in the nonparametric framework and finally the challenges for implementation of the TF framework to the CPF.

G. CPF as CP signal estimator

Originally, the CPF is proposed for parametric estimation of the CP signal ($P = 3$). The CPF applied on the third-order PPS equals

$$C(t, \Omega) = A^2 e^{j2\sum_{p=0}^3 a_0 t^p} \sum_n w(n) e^{j(2(a_2 + 3a_3 t) - \Omega)n^2}. \quad (31)$$

As it can be seen, (31) is concentrated on the CR of the CP signal, $\Omega(t) = \phi''(t) = 2(a_2 + 3a_3 t)$. The two the highest-order parameters, a_2 and a_3 , are estimated from the CPF calculated in two instants, $t = 0$ and $t = t_1$:

$$\begin{aligned} \hat{\Omega}(t) &= \arg \max_{\Omega(t)} |C(t, \Omega)|^2, \\ \hat{a}_2 &= \frac{1}{2} \hat{\Omega}(0), \\ \hat{a}_3 &= \frac{1}{6t_1} [\hat{\Omega}(t_1) - \hat{\Omega}(0)]. \end{aligned} \quad (32)$$

The other parameters can be estimated after dechirping signal (3), where $P = 3$, with $\exp(-j\hat{a}_2 n^2 - j\hat{a}_3 n^3)$:

$$\begin{aligned} y_d(t) &= y(t) \exp(-j\hat{a}_2 n^2 - j\hat{a}_3 n^3) \\ Y(\omega) &= \text{FT}\{y_d(t)\} \\ \hat{a}_1 &= \arg \max_{\omega} |Y(\omega)| \\ \hat{a}_0 &= \angle Y(a_1), \quad \hat{A} \propto |Y(a_1)|. \end{aligned} \quad (33)$$

The CPF is only unbiased for the CP signal with MSEs of signal parameters given in the following [89], [108], [109]:

$$\begin{aligned} \text{MSE}\{\hat{a}_3\} &= \left(1.455 + \frac{1.32}{\text{SNR}}\right) \left[\frac{1400}{\text{SNR} \cdot N^7}\right] \\ &= \left(1.455 + \frac{1.32}{\text{SNR}}\right) \text{CRLB}\{\hat{a}_3\}, \end{aligned} \quad (34)$$

$$\begin{aligned} \text{MSE}\{\hat{a}_2\} &= \left(1 + \frac{1}{2\text{SNR}}\right) \left[\frac{90}{\text{SNR} \cdot N^5}\right] \\ &= \left(1 + \frac{1}{2\text{SNR}}\right) \text{CRLB}\{\hat{a}_2\}, \end{aligned} \quad (35)$$

$$\begin{aligned} \text{MSE}\{\hat{a}_1\} &= \left(1.385 + \frac{1.1}{\text{SNR}}\right) \left[\frac{37.5}{\text{SNR} \cdot N^3}\right] \\ &= \left(1.385 + \frac{1.1}{\text{SNR}}\right) \text{CRLB}\{\hat{a}_1\}, \end{aligned} \quad (36)$$

$$\begin{aligned} \text{MSE}\{\hat{a}_0\} &= \left(1 + \frac{0.278}{\text{SNR}}\right) \left[\frac{1.125}{\text{SNR} \cdot N}\right] \\ &= \left(1 + \frac{0.278}{\text{SNR}}\right) \text{CRLB}\{\hat{a}_0\}, \end{aligned} \quad (37)$$

$$\text{MSE}\{\hat{A}\} = \left[\frac{\sigma^2}{2N}\right] = \text{CRLB}\{\hat{A}\}. \quad (38)$$

Compared with the HAF, the CPF has significantly better performance. Note also that the MSE is minimized for $t_1 \approx 0.11N$ samples. Accuracy in estimation of a_3 is above the CRLB for 1.6dB, while for estimation of a_2 it almost reaches to the CRLB for high SNR.

The computational complexity of this technique is approximately $O(2N^2)$ (here 2 is used to emphasize that the CPF should be evaluated in 2 time instants). Note that it cannot be evaluated using FFT algorithms [118], [119], but some attempts to decrease calculation complexity of this and related transforms will be reviewed in Section III-C.

H. Non-parametric CR estimator

The CPF can be used as non-parametric CR estimator as given in (30). When it is applied to FM signals different from the CP signal, this estimator is biased with bias proportional to uncompensated even higher-order phase terms in the auto-correlation $r_{yy}(t, n) = y(t+n)y(t-n)$. The bias is, under assumptions of the small sampling interval $\Delta t \rightarrow 0$ and relatively large number of available samples within the window $N \gg 1$, derived in [82], [120] and it equals to

$$E\{\Delta\hat{\Omega}(t)\} \approx 2A^4\phi^{(4)}(t)N^6(\Delta t)^6[F_6F_0 - F_2F_4], \quad (39)$$

where F_i is parameter depending only on the selected window function in (28), $F_k = \int_{-1/2}^{1/2} w(t)t^k dt$. It can be seen that the bias depends on even-order phase derivatives (here approximated with the fourth-order derivative), while it increases with the window width (it can be seen that this increase is significant). The variance caused by the noise in the CR estimation is derived in [88]

$$E\{[\Delta\hat{\Omega}(t)]^2\} = \frac{360}{\pi^2 N^5 \text{SNR}} \left(1 + \frac{1}{2\text{SNR}}\right) \approx \frac{360}{\pi^2 N^5 \text{SNR}}. \quad (40)$$

From these asymptotic expressions it can be easily concluded that the variance is decreasing in fast manner with window length. From these consideration it follows that there is an optimal window width producing the minimal MSE equal to:

$$\text{MSE}\{\Delta\hat{\Omega}(t)\} = E\{[\Delta\hat{\Omega}(t)]^2\} + E^2\{\Delta\hat{\Omega}(t)\}, \quad (41)$$

giving trade-off between the bias and variance. Currently the algorithm able to determine a trade-off between bias and variance is available only for high SNRs ($\text{SNR} \geq 10\text{dB}$) [120]-[124].

Example 1. For an illustrative example, we consider a sinusoidal FM signal $x(t) = \exp(j12 \sin(2\pi t))$ within interval $t \in [-1, 1]$ with sampling time $\Delta t = 1/256$. Figure 1(a) depicts the absolute value of the CPF with a small window size of 5 samples $h = 5\Delta t$, while the CPF with a large window size of 256 samples is depicted in Figure 1(b). The CR estimate shown in Figure 1(c) from the narrow-window CPF (dashed line) is perfectly located at the true CR value (solid line) even if the CPF is rather spread in this case. The CR estimate from the wide-window CPF (thick line) is influenced by the bias. The second row represents the same CPFs and the CR estimates as in previous example except the noise variance of $\sigma^2 = 0.5$. It can be seen that, in Fig. 1 (d), the time-CR representation of the sinusoidal FM signal is not recognizable for the small window size of 5 samples while the CPF with the large window size of 256 samples still gives accurate results. For this noise amount we have checked the MSE in the estimation and it is shown in Figure 1(g) that the MSE is high for narrow windows due to emphatic noise influence, then gradually decreases toward optimal value and then increases due to bias influence.

I. Differences between CPF and TF representations

The structure of the CPF is similar to that of the TF representations, for example the WD. However, there are numerous issues that are well known and addressed in the TF signal analysis but not quite clear in the time-CR domain. First and probably the most important issue is related to the multicomponent signals. For the TF analysis this issue is well known and addressed with well studied geometry of auto- and cross-terms in the TF and the ambiguity domains [125].

It seems that only some projection and decomposition strategies can be applied to the considered problem but some TF concepts are not directly applicable to the time-CR domain [126]–[129]. A simple peeling strategy is applicable for signals of rather different magnitude. There are no many alternatives in the field to such technique. One of potential sources of difficulty is in the fact that the CPF is not real-valued and that it is fact oscillatory and spread in the time-CR plane.

The second issue is that in the TF analysis there are huge number of available generalization of the WD and related techniques. Many of these techniques are grouped in important classes such as Cohen class of distribution, but also higher-order TF representation, reassigned distributions, adaptive optimal kernel distribution, locally adaptive directional TF representations, etc., [58], [59], [95], [125]– [143]. However, until now there is no any available systematic class of the

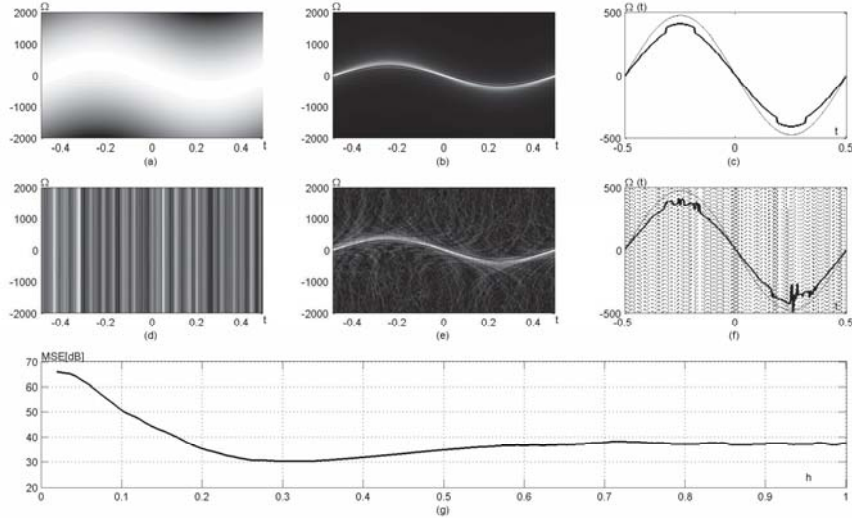


Fig. 1. CR estimation for sinusoidal FM signal: (a) CPF, nonnoisy signal, narrow window; (b) CPF, nonnoisy signal, wide window; (c) comparison of the CR estimates for nonnoisy signal (solid line - true value, dashed line - estimate with narrow window, thick line - estimate with wide window); (d) CPF, noisy signal, narrow window; (e) CPF, noisy signal, wide window; (f) comparison of the CR estimates for noisy signal (solid line - true value, dashed line - estimate with narrow window, thick line - estimate with wide window); (g) MSE in CR estimation for noisy signal as function of the window width.

time-CR domain transforms with a notable approach available in [144].

The third issue is connection with the popular fractional Fourier transform (FrFT) [145]- [150]. At the first glance it is similar to the CPF with quadratic phase term in the integral or sum. The FrFT is a linear transform but there is no any established relationship between the CPF and the FrFT like in the TF analysis between the short-time Fourier transform (STFT) and high-order TF representations [151], [152].

Also, there is no progresses in development for improving concentration in the time-CR domain which parallels the reassigned distribution for the TF analysis [136]- [141].

From the above observations it is not difficult to conclude that a direct generalization and usage of numerous tips and tricks developed in the TF analysis is not straightforward for the time-CR plane so challenges remain to be addressed.

III. EXTENSIONS OF THE CPF

The CPF is initially proposed for monocomponent CP signals, corrupted by Gaussian noise motivated by problems in the passive radar surveillance and echolocation. This limitation motivated researchers to actively look for the CPF modification that is able to address some of the following issues: higher-order PPS, multicomponent signals, non-Gaussian noise, etc. In the following subsections we summarize developments along these lines.

In Section III-A extensions of the CPF with higher-order nonlinearity are presented, while Section III-B describes the hybrid (P)HAF-CPF approach. Section III-C summarizes non-uniform sampling techniques related to the CPF. Projection based techniques are described in Section III-D, while multidimensional transforms are presented in Section III-E. The CPF modification that is robust to the impulse noise is reviewed in Section III-F, while technique for efficient refinement of the CR estimates are given in Section III-G. Problem of

time-CR representation of multicomponent signals is presented in Section III-H while the CPF application in the case of downsampled data is discussed in Section III-I. The Viterbi algorithm (VA) for the IF and CR estimation in high-noise environment is presented in Section III-J. Section is concluded with numerical examples and performance evaluation of considered techniques.

A. High-order (nonlinearity) transforms

The term high-order is often used in the nonstationary signal analysis in an ambiguous manner. There are several tools claiming that they are high- (or higher) order, while showing quite different developments. Therefore, in this subsection, with nonlinear transform we assume the high-order transform as the one involves the product of more than two time-shifted signal terms (more than one auto-correlation) in the sum or integral.

Nonlinear transforms have been already used in the TF analysis. The generalized higher-order TF representation can be written as [132], [133]

$$\text{TF}(t, \omega) = \sum_n w(n) \left[\prod_{i=1}^I r_{yy}^{d_i}(t, c_i n) \right] \exp(-j2\omega n), \quad (42)$$

where $\{c_i, d_i | i \in [1, I]\}$ are selected in such a way that $\text{TF}(t, \omega)$ is concentrated on the IF with eliminated high-order phase derivatives (see eq.(25)). In the WD case (22), $r_{yy}(t, c_i n) = y(t + c_i n)y^*(t - c_i n)$. By using the Taylor series expansion of the phase function, it can be shown that the TF representation is concentrated on the IF if the following condition is satisfied

$$\sum_{i=1}^I r_i c_i = 1. \quad (43)$$

In addition, the high-order odd phase derivatives of the product

TABLE I
SOME REPRESENTATIVES FROM THE HIGH-ORDER CPF CLASS.

$2R$	r_i	c_i
2	1	1
4	2	$\sqrt{2}/2$
6	(1,1,-1)	(1.2646,1.3544,1.5600)
6	(1,1,-1)	(1.0875,1.9333,1.9800)
8	(1,1,-1,-1)	(1.4759,2.9432,2.9800,0.9800)

in (42) are equal to zero when

$$\sum_{i=1}^I r_i c_i^{2p+1} = 0, p = 1, 2, \dots, R. \quad (44)$$

For a given R , we have up to $2R + 1$ phase coefficients eliminated from the product of auto-correlations. Transforms from this group form a popular class of the higher-order TF representations known as the polynomial Wigner-Ville distributions (PWVD) [132], [133]. The popular form of the PWVD is

$$\text{PWVD}(t, \omega) = \sum_n r_{yy}^2(t, 0.675n) r_{yy}^*(t, 0.85n) e^{-j2\omega n}. \quad (45)$$

It is concentrated on the IF for the PPS of the fifth order. Evaluation of $\text{PWVD}(t, \omega)$ requires interpolation of the signal samples (see more details in Section III-C where the general non-uniform sampling and signal interpolation strategies have been considered).

The same principle has been utilized to extend the CPF for the high-order PPS to concentrate on the CR while cancelling other even-order phase derivatives [153], [154]:

$$H(t, \Omega) = \sum_n \left[\prod_{i=1}^I r_{yy}^{(r_i)}(t, c_i n) \right] \exp(-j\Omega n^2). \quad (46)$$

Comparing relations (42) with (46), two differences are noticeable. Firstly, the auto-correlation in this case is defined as in the CPF (28), (29), $r_{yy}(t, c_i n) = y(t + c_i n)y(t - c_i n)$, while power r_i in brackets in exponent means potential usage of complex conjugates, i.e., $q^{(r_i)} = q^{r_i}$ for $r_i > 0$, and $q^{(r_i)} = (q^*)^{|r_i|}$ for $r_i < 0$. Secondly, parameters $\{c_i, r_i | i \in [1, I]\}$ are chosen according to different conditions

$$\sum_{i=1}^I r_i c_i = 1 \quad (47)$$

$$\sum_{i=1}^I r_i c_i^{2p} = 0, p = 1, 2, \dots, R. \quad (48)$$

The first condition of (47) is to guarantee the concentration on the CR of the signal, while the second condition of (48) is to cancel the higher-order even phase derivatives. The selection of R eliminates up to $2R$ phase-orders from the result of auto-correlations. Note that for selected R , more than one solution may exist. Table I summarizes notable representatives of transforms from this class.

It should be noted that this design brings some undesired effects. Firstly, if the considered signal has the phase order higher than assumed, higher-order phase derivatives may be amplified. These uncompensated derivatives are commonly amplified in high-order representations [133]. The second problem is that high-order nonlinearity causes significant increase of the noise influence (substantial increase of both the

MSE and SNR threshold). In addition, for multicomponent signals, each auto-correlation produces additional cross-terms and it becomes difficult to recognize signal components from the mixture.

When parametric estimation is concerned this transform is calculated at $(P - 1)$ different time-instants. Then, phase parameters are obtained by interpolating the transform position maxima using the least-squares interpolation. Some details on this strategy can be found in [154].

An alternative high-order technique is the Farquharson-O'Shea-Ledwich approach from [70]. It designs the kernel suitable to the considered PPS order multiplied with the complex exponential of the appropriate form. These high-order transforms can be described as:

$$\text{HP}(t, \Omega) = \sum_n \prod_{i=1}^I r_{yy}^{(r_i)}(t, n c_i / c_{\max}) e^{-j \frac{\Omega p n^p}{c_{\max}^p}}, \quad (49)$$

where c_{\max} is the maximum lag $c_{\max} = \max\{c_i\}$. Detailed analysis of the high-order phase function is performed in [70] including the optimal selection of the lag parameters. These high-order representations and estimators inevitable increase the MSE and SNR threshold. As shown in [70] and [154], the SNR threshold for the PPS signal with the order of $P = 4$ and $P = 5$ is found to be 5dB. This approach is extended to signals with hybrid sinusoidal (nonpolynomial) modulation in [155].

Calculation complexity of this technique is of order $O(kN^2)$ where k is the number of instants required for evaluation of the high-order transforms. There is additional complexity related to more auto-correlations but its complexity is lower than $O(IN)$.

B. (P)HAF-CPF

The hybrid HAF-CPF approach is proposed as an alternative to handle the problem of parameter estimation of high-order PPSs [101], [102]. This technique calculates the PD as in the HAF estimator until the CP signal is obtained. Furthermore, parameters of the obtained signal are estimated by the CPF. This procedure reduces estimators nonlinearity improving the estimation performance with respect to the HAF. Detailed description of the HAF-CPF approach is given in the following.

The PD procedure (11)-(12) is performed $(P - 3)$ times until the CP signal is obtained

$$\begin{aligned} \text{PD}^{P-3}[n, \tau_1, \dots, \tau_{P-3}] &= A^{2^{P-3}} e^{j c_3 a_P n^3 + j c_2 a_{P-1} n^2} \\ &\quad \times e^{j(c_1 a_{P-2} + c_1' a_P) n + j(c_0 a_{P-3} + c_0' a_{P-1})} \\ &\quad + \nu_x(n), \end{aligned} \quad (50)$$

where c_i , $i = 2, 3$, c_i' , c_i'' , $i = 0, 1$, are constants dependent only on P and selected set of lags $\{\tau_i, i \in [1, P-3]\}$. Two the highest-order phase coefficient of signal (50), a_P and a_{P-1} , are estimated by the CPF

$$\begin{aligned} C_y(t, \Omega) &= \sum_k \text{PD}^{P-3}[t + n, \tau_1, \dots, \tau_{P-3}] \\ &\quad \times \text{PD}^{P-3}[t - n, \tau_1, \dots, \tau_{P-3}] e^{-j\Omega n^2}, \end{aligned} \quad (51)$$

evaluated in two instants:

$$\hat{a}_P = \frac{\hat{\Omega}(t_1) - \hat{\Omega}(0)}{6t_1c_3}, \quad (52)$$

$$\hat{a}_{P-1} = \frac{\hat{\Omega}(0)}{2c_2}, \quad (53)$$

where $\hat{\Omega}(t) = \arg \max_{\Omega} |C_y(t, \Omega)|$. The lower-order coefficients can be estimated from dechirped signal $\tilde{y}(n) = y(n) \exp(-j\hat{a}_P n^P - j\hat{a}_{P-1} n^{P-1})$. The selection of lag parameters and t_1 is discussed in [101] with optimal values $\tau^{\text{opt}} = \tau_1 = \tau_2 = \dots = \tau_{P-3} \approx \lceil (-0.006P + 0.107)N \rceil$, and $t_1^{\text{opt}} \approx \lceil (0.0254 + 1.4474e^{-0.7305P})N \rceil$. Details related to realization and alternatives are given in [101]. Reduction of number of auto-correlations with respect to the HAF brings significant benefits in terms of both MSE and SNR threshold. The SNR threshold is reduced with respect to the HAF for about 9.5dB [101].

Following the same reasons as in development of the PHAF, the parameters of multicomponent signals can be estimated from the product of several hybrid HAF-CPFs calculated with different lag sets

$$\text{PC}_y(t, \Omega) = \prod_{l=1}^L |C_y^l(t, \Omega)|, \quad (54)$$

$$C_y^l(t, \Omega) = \sum_n \text{PD}^{P-3}[t + n, \tau_1^{(l)}, \dots, \tau_{P-3}^{(l)}] \times \text{PD}^{P-3}[t - n, \tau_1^{(l)}, \dots, \tau_{P-3}^{(l)}] e^{-j\Omega F_l n^2}, \quad (55)$$

where $F_l = \prod_{i=1}^{P-3} \tau_i^{(l)} / \tau_i^{(1)}$ is the scaling operator and L is the number of different sets of lags. The resulting function is referred to as the product HAF-CPF (PHAF-CPF). Due to different lags in (55), the cross-terms appear at different locations for different l , while the auto-terms are distributed along the same location. Therefore, the product (54) attenuates the cross-terms and enhances the auto-terms. Furthermore, the two highest-order phase parameters of each component can be estimated by locating M peaks of the PHAF-CPF at two time instants. In the same manner as the PHAF in addition to elimination of cross-terms attenuates noise influence with respect to the HAF the PHAF-CPF attenuates both interference components and noise influence with respect to the HAF-CPF.

C. Nonuniform sampling techniques

One obvious issue of the CPF is its calculation complexity. Namely, the CPF cannot be evaluated by the FFT algorithms since its definition does not include complex exponential with linear phase term but instead it has exponential with quadratic phase term $\exp(-j\Omega n^2)$. There are some strategies for fast evaluation of the polynomial FT [156], [157], [158], [159]. However, they have numerous limitations preventing their simple application to the wideband PPS signals.

The potential strategy to address this issue is to nonuniform sample the continuous signal (referred to as the NU-CPF here) [104]:

$$\begin{aligned} C'(t, \Omega) &= 2 \sum_{m=0}^{n_{\max}} y(t + \sqrt{cn})y(t - \sqrt{cn})e^{-j\Omega n} \\ &= 2 \sum_{m=0}^{n_{\max}} r_{yy}(t, \sqrt{cn})e^{-j\Omega n}, \end{aligned} \quad (56)$$

where n_{\max} is maximal possible value of the time-lag n . For example if t is in the middle of the available interval and we have $N/2$ samples from both sides ($N + 1$ in total) then $\sqrt{cn_{\max}} < N/2$, i.e., $n_{\max} \leq N^2/4c$. For some particular instant t , $n_{\max} \leq (N/2 - |t|)^2/c$. It is recommended that the constant c is selected so that all signal samples from the basic interval are included, i.e., $c = N/2$.

It is easy to see the benefit of the non-uniform sampling since there is linear complex exponential in sum giving possibility to evaluate this transform using the FFT. However, the remaining question is availability of nonuniformly spaced samples. It is rare to have nonuniformly sampled signals and it is more difficult to have nonlinear sampling in this form. Therefore, we have to interpolate available (usually uniformly sampled) data. Papers [6], [104] proposed to use the interpolation strategy based on the FT of signal zero-padded in the time domain by factor 4 or 8. After interpolation using zero-padding, obtained grid has FN samples where F is upsampling factor ($F = 4$ or $F = 8$ are recommended) (see Section III-I). If considered sample n_j is not on this denser grid and two closest neighbors are n_i and n_{i+1} , $n_j \in (n_i, n_{i+1})$ then signal can be interpolated as

$$\tilde{y}(n_j) = \hat{y}(n_i)F[n_j - n_i] + \hat{y}(n_{i+1})F[n_{i+1} - n_j]. \quad (57)$$

In several papers this simple and effective technique shows negligible accuracy reduction with respect to the standard CPF form [6], [88], [104], [105].

For high-order PPS there are several potential tools where the nonuniform sampling can be utilized. One is to employ the hybrid HAF-CPF technique for reducing to the CP signal and then to evaluate nonuniformly sampled form of the CPF. For details refer to [104].

In [6], it has been shown that the combination of the auto-correlations and nonuniform sampling can significantly improve estimation results for higher-order PPS. A prominent representative of this class of estimator can be described as:

$$G(t, \Omega) = 2 \sum_{m=0}^{n_{\max}} r_{yy}^*(t, \sqrt{cn})r_{yy}(t, \sqrt{cn + \tau})e^{-j4\Omega\tau cn}, \quad (58)$$

where the scaling factor c is selected as previously described. For the fifth-order PPS ($P = 5$), $G(t, \Omega)$ is concentrated along the line $\Omega = a_5 t + a_4$. Therefore, estimation of two highest-order parameters can be performed as in the CPF, by evaluating $G(t, \Omega)$ at $t = 0$ and $t = t_1$ and performing the least-square interpolation as in the case of the CPF (31), (32). In this way, estimation of two highest-order parameters, a_5 and a_4 , is performed. The lower-order parameters can be estimated after the signal dechirping considering the obtained signal $y_3(n) = y(n) \exp(-j\hat{a}_5 n^5 - j\hat{a}_4 n^4)$. More elaborated procedure based on the non-uniform sampling is proposed in [6] for a seventh-order PPS.

D. Projection based techniques

When multicomponent signals are considered, the CPF is influenced by cross-terms that usually mask auto-terms making parameter estimation difficult. The cross-terms influence can be significantly reduced by projecting the CPF for various

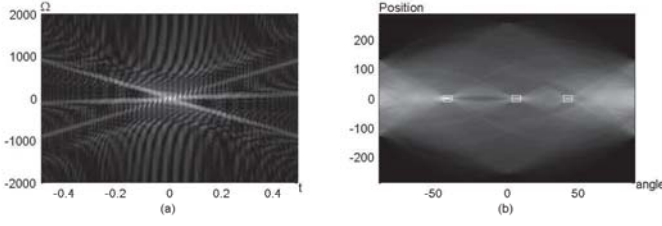


Fig. 2. Sum of three CP signals: (a) CPF; (b) Radon transform of the CPF, white rectangles represents peaks corresponding to the signal components.

time instants t . Obtained CPF is then summed and oscillatory effect in the CPF auto-terms (it is important disadvantage with respect to the TF representation where only cross-terms oscillate) are partially compensated in addition to eliminating the cross-terms.

A particularly simple estimator of the second-order PPSs is proposed in [160] and is referred to as the integrated CPF, where $C(t, \Omega)$ is calculated for various instants t and obtained values are summed

$$C(\Omega) = \sum_t |C(t, \Omega)|^2. \quad (59)$$

This estimator has shown to concentrate on the CR of components with results comparable with the Radon WD and related projection techniques in the TF plane [126], [127], [128]. Similar projections can be used for the CR estimation refinement for the case of CP signals [160]- [167].

Example 2. Considered the sum of three CP signals

$$x(t) = e^{j12\pi t^3 - j24\pi t} + e^{j96\pi t^3 + j24\pi t} + e^{-j96\pi t^3 - j24\pi t}, \quad (60)$$

where $t \in [-1, 1]$ with sampling time $t \in 1/256$. The CPF of (60) is depicted at Figure 2(a) where oscillatory nature of auto-terms can be observed. The Radon transform calculated for this image is given in Figure 2(b). Three peaks corresponding to positions of signal components are denoted with white rectangles.

E. High-order (multidimensional) CPF

For the parameter estimation, higher-order phase terms are compensated by increasing the kernel order (see Section III-A). It inevitably leads to deterioration of the algorithm performance since it is well known that the high-order kernels cause more noise influence and increase both the SNR threshold and MSE. Alternative approach is to keep kernel like in the CPF but to perform search over multidimensional parameters space (emphasized in the title of this subsection) [103]

$$HC(t; \Omega_2, \dots, \Omega_P) = \sum_n y(t+n)y(t-n)e^{-j \sum_{p=1}^{\lfloor P/2 \rfloor} \Omega_{2p} n^{2p}}, \quad (61)$$

where $\lfloor \cdot \rfloor$ is operator rounding to smaller integer. This approach is referred to as the high-order CPF (HO-CPF) and it is ideally concentrated on even-order phase derivatives of the signal phase, $\Omega_{2p} = \phi^{(2p)}(t)$ for $p \leq P/2$. By evaluating $HC(t; \Omega_2, \dots, \Omega_P)$ at two instants, $t = 0$ and $t = t_1$, all phase parameters a_p , $p \leq P$ are obtained.

The high-order WD (HO-WD) is a similar tool that is used in the TF and it is defined as [166]

$$HW(t; \omega_1, \dots, \omega_P) = \sum_n y(t+n)y^*(t-n)e^{-j2 \sum_{p=1}^{\lfloor P/2 \rfloor} \omega_p n^{2p-1}}. \quad (62)$$

In the case of noise free signals, the HO-WD is concentrated on odd-order phase derivatives $\omega_p = \phi^{(2p-1)}(t)$, $2p-1 \leq P$. Again, the P th order PPS coefficients can be estimated from the HO-WD evaluated at two instants. However, when the HO-CPF or HO-WD are evaluated at two instants, signal parameters estimation requires elaborate expression and obtained results are sometimes significantly above the CRLB.

A useful observation is that the HO-CPF can be used for estimation of even-order phase derivatives while the HO-WD can be used for estimation of odd-order derivatives [103], [105]. It has been shown that it is possible to calculate $HC(0; \Omega_2, \dots, \Omega_P)$ and $HW(0; \omega_1, \dots, \omega_P)$ both in origin for $t = 0$ and that position of the maxima of these transforms corresponds to the parameters of the PPSs. Evaluation in the origin means that the signal length in corresponding transforms is not reduced. In addition, signal parameters are in both cases directly available without need for elaborate expressions. Therefore we can estimate coefficients as:

$$(\hat{a}_2, \hat{a}_4, \dots, \hat{a}_Q) = \arg \max_{(\Omega_2, \dots, \Omega_Q)} |HC(0; \Omega_2, \dots, \Omega_Q)| \quad (63)$$

$$(\hat{a}_1, \hat{a}_3, \dots, \hat{a}_R) = \arg \max_{(\omega_1, \dots, \omega_R)} HW(0; \omega_1, \dots, \omega_R), \quad (64)$$

where (Q, R) are given as

$$(Q, R) = \begin{cases} (P, P-1), & P \text{ even} \\ (P-1, P), & P \text{ odd.} \end{cases}$$

For PPS of the order higher than $P \geq 5$ search over parameters space higher than 2 is required, i.e., complexity of these transforms is $O(N^{\lceil P/2 \rceil})$ where $\lceil \cdot \rceil$ is operator rounding to larger integer. Instead of the direct search optimization is commonly performed using the genetic algorithm (GA) or some other metaheuristic strategy [79]. This strategy has higher complexity than the CPF and (P)HAF-CPF but accuracy is better and the SNR threshold lower than in these counterparts. Simulations are given in Section III-K.

F. Robust CPF

The CPF is designed for the Gaussian noise environment but it is sensitive to the impulse noise influence. Accurate CR estimation and signal representation in the time-CR domain is of a high importance for signals corrupted by impulsive noise.

Assuming that $w(n) = 1/(N+1)$ for $n \in [-N/2, N/2]$ and $w(n) = 0$ elsewhere, the CPF given by (29) can be written in an alternative form:

$$C(t, \Omega) = \text{mean}\{|r_{yy}(t, n)e^{-j\Omega n^2}|\}, n \in [-N/2, N/2] \quad (65)$$

As it can be seen from (65), in calculation of the average value, all samples of modulated auto-correlation $r_{yy}(t, n) \exp(-j\Omega n^2)$ are taken with equal weights. Therefore, those corrupted with impulse noise will significantly disturb the result of averaging and at the same time lower the accuracy of the CPF [63], [167], [168], [169]. Therefore,

the robust CPF is proposed in [167] by introducing the L-filter form of the CR estimator:

$$\mathbf{C}_L(t, \Omega) = \sum_{l=-N/2}^{N/2} a_l [\mathbf{r}_{(l)}(t, \Omega) + j\mathbf{i}_{(l)}(t, \Omega)] \quad (66)$$

where $\mathbf{r}_{(l)}(t, \Omega) \in \mathbf{R}(t, \Omega)$ and $\mathbf{i}_{(l)}(t, \Omega) \in \mathbf{I}(t, \Omega)$. Sets $\mathbf{R}(t, \Omega)$ and $\mathbf{I}(t, \Omega)$ are formed as:

$$\mathbf{R}(t, \Omega) = \{\text{Re}\{r_{yy}(t, n)e^{-j\Omega n^2}\} | n \in [-N/2, N/2]\}, \quad (67)$$

$$\mathbf{I}(t, \Omega) = \{\text{Im}\{r_{yy}(t, n)e^{-j\Omega n^2}\} | n \in [-N/2, N/2]\}, \quad (68)$$

Elements $\mathbf{r}_{(l)}(t, \Omega)$ and $\mathbf{i}_{(l)}(t, \Omega)$ from the corresponding sets are sorted into a non-decreasing order:

$$\mathbf{r}_{(l)}(t, \Omega) \leq \mathbf{r}_{(l+1)}(t, \Omega), \quad \mathbf{i}_{(l)}(t, \Omega) \leq \mathbf{i}_{(l+1)}(t, \Omega). \quad (69)$$

Weights of the L-filter are selected as: $\sum_{l=-N/2}^{N/2} a_l = 1$ (energy condition) and $a_l = a_{-l}$ (unbiasedness condition). Commonly the α -trimmed CPF is used [63], [167], with $a_l = 1/(2Na + 1)$ for $l \in [-aN, aN]$ and $a_l = 0$ elsewhere in (66). For $a = 1/2$ the standard CPF (65) is obtained, while for $a \in [0, 1/2)$, we obtain the robust form where some percentage of the samples with the highest magnitudes are removed. However, obtained technique suffers from a low breakdown point which inspired research efforts in order to improve its robustness against impulse noise.

The impulse noise influence can be further reduced by signal filtering using the robust DFT. The robust DFT with high breakdown point can be calculated as [63], [68], [168]

$$\hat{Y}(\omega) = \hat{Y}_1(\omega) + \hat{Y}_2(\omega) + j[\hat{Y}_3(\omega) + \hat{Y}_4(\omega)], \quad (70)$$

$$\hat{Y}_i(\omega) = \sum_{l=-N/2}^{N/2} a_l \mathbf{y}_{(i,l)}(\omega) \quad (71)$$

where $\mathbf{r}_{(i,l)}(\omega)$ are sorted elements from the sets:

$$\mathbf{y}_{(i,l)}(\omega) \in \mathbf{R}_i(\omega) = \{y_i(n, \omega)\}, \quad i = 1, 2, 3, 4, \quad (72)$$

with $y_1(n, \omega) = r(n) \cos(\omega n)$, $y_2(n, \omega) = i(n) \sin(\omega n)$, $y_3(n, \omega) = -r(n) \sin(\omega n)$, and $y_4(n, \omega) = i(n) \cos(\omega n)$, where $r(n) = \text{Re}\{y(n)\}$ and $i(n) = \text{Im}\{y(n)\}$. Then, the standard CPF (65) is calculated for the signal obtained using standard inverse FT, $\hat{y}(n) = \text{IFT}\{\hat{Y}(\omega)\}$.

Example 3. In this example a mono-component CP signal is considered

$$x(t) = \exp(j96\pi t^3 + j24\pi t), \quad (73)$$

within interval $t \in [-1, 1]$ with sampling time $\Delta t = 1/256$. The standard and robust CPF of this signal are depicted in Figures 3(a) and (b) and from both plots these time-CR domain representations of the CP signal can be recognized. However, when the considered signal is corrupted by the impulse noise then the standard CPF fails to reveal reliable information on the signal (Figure 3(c)) while signal component still can be easily recognized from the robust CPF (Figure 3(d)).

G. Refinement of the CPF estimators

Precise estimation of PPS parameters by direct evaluation of the CPF (or related estimators) requires calculation of estimator's function over dense grid of CR values. Therefore, in order to reduce the computational complexity, a parameter

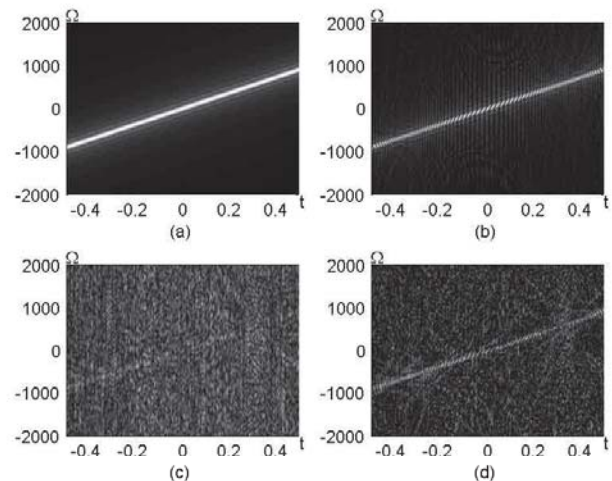


Fig. 3. Time-CR representations of the cubic phase signal: (a) the standard CPF of noise-free signal; (b) the robust CPF of noise-free signal; (c) the standard CPF of signal corrupted by impulsive noise; (d) the robust CPF of signal corrupted by impulsive noise.

refinement strategies are used. All of them have common initial stage in which the CPF is evaluated over coarse grid of the CR values and initial coarse estimate Ω_c is obtained.

The coarse estimate Ω_c can be refined using dichotomous (binary) search [170], [171]. The algorithm starts with the selection of the width of considered search interval $\Delta\Omega$ that equals the coarse grid resolution. Then, the CPF (or some similar related transform) is evaluated at two points $\mathbf{C}_{\pm 1} = \mathbf{C}(n, \Omega_c \pm \Delta\Omega/2)$ and $\Omega_m = \Omega_c$. Further, the following steps are repeated several times:

Step 1. Reduce the width of search interval

$$\Delta\Omega \leftarrow \Delta\Omega/2. \quad (74)$$

Step 2. Evaluate $\mathbf{C}_{\pm 1} = \mathbf{C}(n, \Omega_m \pm \Delta\Omega/2)$ and update Ω_m :

$$\Omega_m \leftarrow \begin{cases} \Omega_m + \Delta\Omega & |\mathbf{C}_1| > |\mathbf{C}_{-1}| \\ \Omega_m - \Delta\Omega & |\mathbf{C}_{-1}| > |\mathbf{C}_1| \end{cases}. \quad (75)$$

After Q iterations, final estimate is obtained as $\hat{\Omega}(n) = \Omega_m$.

Note that, in the case of the CPF and related transforms with non-linear complex exponential terms efficient strategies, such as Aboutanous-Mulgrew technique cannot be used [172], [173]. However, in the case of nonuniform sampled data with linear term in the phase exponential, this strategy can be conducted. For more details refer to [170], [171], [174].

H. CPF and multicomponent signals

Parameter estimation of multicomponent PPSs,

$$y(t) = \sum_i x_i(t) + \nu(t), \quad (76)$$

are usually performed on two ways:

- 1) When signal components $x_i(n)$ differ in magnitudes, the strongest one can be estimated first and peeled from the mixture. Then the similar approach is used for the estimation of the next component. To be more precise, in the following we are giving more details.

The first step of the algorithm is to estimate parameters of the strongest component $\hat{a}_{i,q}$, $i \in [1, P]$ (second index q corresponds to signal component), where $q = 1$, using any described estimator proposed for monocomponent signal. In the second step, signal $y(t)$ is dechirped using parameters of the estimated component $y_d(t) = y(t) \exp\left(-j \sum_{i=0}^P \hat{a}_{i,q} t^i\right)$ and the FT of the resulted signal $Y(\omega) = \text{FT}\{y_d(t)\}$ is calculated. In the third step, $Y(\omega)$ is filtered with high-frequency filter by removing frequencies around $Y(0)$ to obtain $Y_{\text{fil}}(\omega)$. In the fourth step, the inverse FT is performed and signal is modulated to be prepared for the next iteration (search for new component) $y'(t) = \text{IFT}\{Y_{\text{fil}}(\omega)\} \exp\left(j \sum_{i=0}^P \hat{a}_{i,q} t^i\right)$. The next component is estimated from $y'(t)$ and procedure is performed for each signal component. This kind of procedure is common for all previously introduced CPF related transforms.

- 2) When signal components have similar magnitudes, the product-based transforms are currently best available solutions (see the PHAF-CPF, Section III-B). While evaluating these transforms, the lags sets should be selected in such a way that auto-terms are located on the same position while the cross-terms are located on different places. Therefore, the followed multiplication amplifies auto-terms and in the same time suppresses cross-terms.

An alternative to these two approaches is to perform projection of the CPF or related transform along CR in order to attenuate effect of cross-terms as discussed in Section III-D.

Finally, when the goal is nonparametric estimation of multicomponent signals and obtaining accurate TF or time-CR representations of signal components, signal decomposition can be applied. For example, in [175], signal decomposition combining TF representations and time-CR domain analysis has been considered. Signal components decomposition and evaluation of the CPF for each signal component separately is performed using the STFT, defined as

$$\text{STFT}(t, \omega) = \sum_n y(t+n) w^*(n) e^{-j\omega n}. \quad (77)$$

The STFT is a linear transform and cross-terms between components can appear only when they are very close to each other (within window width in the frequency domain) [176]. The inverse STFT can be written as:

$$y(t+n) = \frac{1}{2\pi w^*(n)} \int_{-\infty}^{\infty} \text{STFT}(t, \omega) e^{j\omega n} d\omega. \quad (78)$$

For a sake of simplicity, we assume that the window function within the interval of interest is equal to 1. Substituting (78) in the CPF, we obtain (ignoring multiplicative constants):

$$C(t, \Omega) = \int_{\omega} \int_{\theta} \text{STFT}(t, \omega + \theta) \text{STFT}(t, \omega - \theta) \Pi_{\Omega}(2\theta) d\omega d\theta, \quad (79)$$

where $\Pi_{\Omega}(\cdot)$ is the FT of the linear FM signal $\exp(-j\Omega t^2)$:

$$\Pi_{\Omega}(\theta) = \sum_t \exp(-j\Omega t^2) \exp(-j\theta t). \quad (80)$$

The implementation of the CPF (79) in the time-CR domain is a counterpart of the TF transform called the S-method [151], [176]. Assume now that a significant energy of any signal component exists only within the frequency region $[\omega_{bi}(t), \omega_{ei}(t)]$, and that signal components are non-overlapping in the TF plane, i.e., $[\omega_{bi}(t), \omega_{ei}(t)] \cap [\omega_{bj}(t), \omega_{ej}(t)] = \emptyset$ for $i \neq j$. Then, the CPF for the i th signal component can be written as:

$$C_i(t, \Omega) = \iint_{\omega_{bi}(t) \leq \omega \pm \theta \leq \omega_{ei}(t)} \text{STFT}(t, \omega + \theta) \text{STFT}(t, \omega - \theta) \Pi_{\Omega}(2\theta) d\omega d\theta. \quad (81)$$

In this way, evaluation of the CPF for the i th component $C_i(t, \Omega)$ is separated from evaluation of the CPF for other components. Determination of region of the signal components is non-trivial and it heavily depends on the considered signal type. The Otsu algorithm [177] is used in [175] for adaptive signal components region determination. For closer signal component in the TF plane instead of the STFT some high-resolution TF representation for component separation can be used [178].

I. CPF and undersampled data

One of the most attractive developments in the signal processing is investigation how techniques can be adopted for undersampled signals [179]- [182]. These considerations meet conditions of the so-called compressed sensing framework [183]- [186]. The PPS parameter estimation is not closely related to the Nyquist sampling rate. Namely, the PPS signal is determined by number of parameters that could be significantly smaller than number of samples required by the sampling theorem. Detailed study of the identifiability for the PPS parameters is considered in [48], [110], [111]. Meanwhile, several different approaches are developed for handling PPS estimation of undersampled data with respect to the sampling theorem requirement [18], [28].

In the case of the CPF-related transform, it has been shown that, when signal is sampled symmetrically around the origin (middle of the interval), i.e. that for each sample $y(t + \tau_i)$ exists symmetric counterpart $y(t - \tau_i)$, there is no significant changes in the CPF realization since the CPF can be calculated as

$$\tilde{C}(t, \Omega) = \sum_{i=1}^{N_I} r_{yy}(t, \tau_i) e^{-j\Omega \tau_i^2} = 2 \sum_{i=1}^{N_I/2} r_{yy}(t, \tau_i) e^{-j\Omega \tau_i^2}. \quad (82)$$

The loss of accuracy that is proportional to reduction in number of samples with respect to the number required by the Nyquist rate is expected.

However, in the case when symmetric signal samples $t \pm \tau_i$ are not available, some sort of data interpolation is required. In [179], the following interpolation procedure has been proposed. Firstly, the DFT is approximated from the available samples using the numerical integration technique as

$$Y(p) \approx \frac{1}{T} \sum_{k=1}^{K-1} y(t_k) e^{-j2\pi p t_k} (t_k - t_{k-1}), \quad p \in [-N/2, N/2-1]. \quad (83)$$

Taking the inverse DFT of zero-padded $Y(p)$ with the factor F (commonly $F = 2, 4$ or 8), uniformly sampled version of $y(t)$ is obtained as

$$\hat{y}(t) = \frac{1}{FN} \sum_p Y_z(p) e^{j2\pi p \frac{t}{FN}}, \quad t \in [-FN/2, FN/2], \quad (84)$$

where $Y_z(p)$ is zero-padded $Y(p)$. Now, the aim is to calculate missing samples $y(t_k)$ required for evaluation of the CPF from $\hat{y}(t)$. For this purpose, interpolation formula (84) can be used as in the case of nonuniformly sampled signal. This strategy can also be used in case of the HO-CPF and HO-WD evaluations (42), (49). The alternative interpolation approaches with direct interpolation of the auto-correlation function $r_{yy}(t, \tau_i)$ [187] or matching pursuit strategies [188] can also be employed from instead of interpolation in the time domain.

J. Viterbi algorithm and CPF

When the number of samples is large, the CR can vary in the considered interval. Then, it is inevitable to calculate the CPF for windowed data and to track CR for signal duration. In a high noise environment, a common situation is that the CPF follows the CR in some part of the interval and in other part of the interval produces wrong CR estimates. Therefore, development of the algorithm that is able to follow CR removing instants giving inaccurate estimates is rather important. One such algorithm is developed in [189]. It is inspired by the VA proposed for the IF estimation in the TF analysis [190]- [193].

The CR estimator can be written as a solution to the following optimization problem

$$\hat{\Omega}(t) = \arg \min_{\Omega(n)} \left[\sum_{n=n_1}^{n_2-1} g(\Omega(t), \Omega(t+1)) + \sum_{n=n_1}^{n_2} f(|C(t, \Omega(t))|) \right], \quad (85)$$

where function $f(\cdot)$ is formed by sorting the CPF values for the considered instant. The maximal value is penalized with 0, the second largest is penalized with 1, the third one with value 2, etc. This clearly reflects the idea that even in the high noise environment the CR is on one of the highest values of the CPF. The second function is set as $g(x, y) = \rho(|x - y| - \Delta)$ for $|x - y| > \Delta$, and $g(x, y) = 0$ elsewhere, where ρ is weight of the penalization function, while Δ is threshold above which CR variations between consecutive instants are penalized. Details on the VA implementation can be found in [192].

Obtained CR estimate can be back-projected through the TF representations in order to get precise IF estimate. For FM signal with a cubic modulation, the CPF is concentrated on the CR. However, the TF representations are not concentrated on the IF due to inner interferences and bias [125] for non-linear FM function. In addition, it can be expected that for high-order polynomial FM functions the inner interferences and bias will be smaller in the case of the CPF than for the TF representations. Then, the CR estimate obtained from the VA is used in the IF estimation. In the first step of the algorithm, the VA is performed (85). Then the cumulative sum of obtained

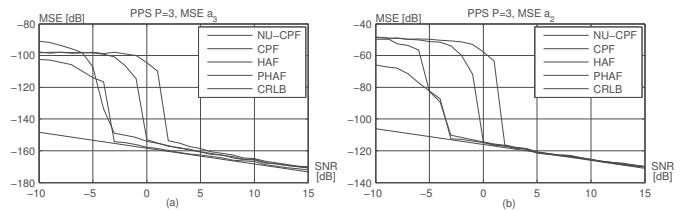


Fig. 4. MSE of the two highest-order phase estimates obtained by the CPF, NU-CPF, HAF, and PHAF-based estimation procedures: (a) MSE of a_3 ; (b) MSE of a_2 .

estimates:

$$\hat{\mu}(t) = \Delta t \sum_{k=t_1}^t \hat{\Omega}(k) \quad (86)$$

can be used to estimate the IF with accuracy up to an additive constant. This constant can be determined as

$$\hat{\mu} = \arg \max_{\mu} J(\mu), \quad (87)$$

$$J(\mu) = \sum_{n=n_1}^{n_2} \text{TF}(t, \hat{\mu}(t) + \mu). \quad (88)$$

The function $J(\mu)$ is greater for lines $\hat{\mu}(t) + \mu$ that are closer to the true IF. Then, the IF estimate can be calculated as $\hat{\omega}(t) = \hat{\mu}(t) + \hat{\mu}$. The accuracy of the IF estimation is improved since the influence of the high-order phase terms is reduced with respect to the VA applied to the TF representations.

K. Examples and comparisons

Example 4. We consider the CPF, NU-CPF, HAF, and PHAF, for the third-order PPS

$$x(n) = \exp \left(j \sum_{i=0}^3 a_i n^i \right),$$

where $\Delta t = 1$, $n \in [-256, 256]$ and a_i is the i th element of the vector $\mathbf{G} = \{0.9, \pi/7, 2.15 \cdot 10^{-4}, 6.42 \cdot 10^{-4}\}$. The SNR is varied from -10 dB to 15 dB at a stepsize of 1 dB. The CPF, NU-CPF, HAF and PHAF are calculated following instructions from [96], [102], [104]. The MSEs of two the highest-order phase estimates (\hat{a}_3 and \hat{a}_2) are shown in Figure 4. From Figure 4, the CPF and NU-CPF have the SNR thresholds at -3 dB, while the SNR thresholds of the HAF and PHAF are at 2 dB and 0 dB, respectively. For estimating parameter a_3 , the NU-CPF has lowest MSE that is on the CRLB above the SNR threshold, while the CPF and PHAF have similar MSE for $\text{SNR} > 0$ dB. For parameter a_2 , MSEs of all methods approach the CRLB.

Example 5. Performance of the HAF, PHAF, HAF-CPF, PHAF-CPF, and combined HO-WD and HO-CPF (HOWD-CPF) estimator, are evaluated on the sixth-order PPS with the following parameters, $n \in [-128, 128]$, $a_0 = 0$, $a_1 = -3(\Delta t)$, $a_2 = 11(\Delta t)^2$, $a_3 = 7(\Delta t)^3$, $a_4 = -5(\Delta t)^4$, $a_5 = 21(\Delta t)^5$, and $a_6 = -15(\Delta t)^6$, $\Delta t = 0.0078$. The PHAF and PHAF-CPF are calculated using four lag sets which elements are chosen following instructions from [96], [102]. Evaluation of the HOWD-CPF requires two 3-D searches that are optimized using the GA with setup given in [19]. The MSEs of a_6 and a_5 estimates are plotted in Figure 5.

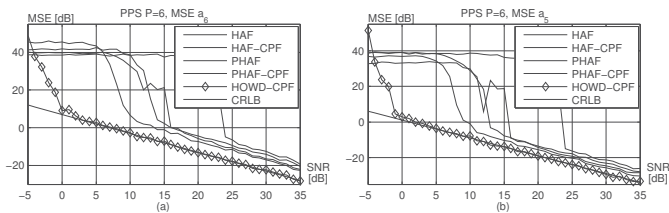


Fig. 5. MSE of the two highest-order phase estimates obtained by the HAF, HAF-CPF, PHAF, PHAF-CPF, and HOWD-CPF-based estimation procedures: (a) MSE of a_6 ; (b) MSE of a_5 .

The SNR thresholds of the HAF, PHAF, HAF-CPF, PHAF-CPF, and HOWD-CPF, are at 24dB, 16dB, 14dB, 10dB, and 0dB, respectively. The HOWD-CPF approaches the CRLB for both parameters, while the MSEs of HAF, PHAF, HAF-CPF, and PHAF-CPF, are more than 10 dB (parameter a_6)/8 dB (parameter a_5), 8 dB (parameter a_6)/6 dB (parameter a_5), 7 dB (parameter a_6)/5 dB (parameter a_5), and 6 dB (parameter a_6)/4 dB (parameter a_5) above the CRLB, respectively.

IV. TWO-DIMENSIONAL PPS

The application of the CPF to 2-D and multidimensional signals is not quite straightforward due to issues related to search dimensions and calculation complexity. In addition, in many practical applications, the 2-D PPS has fast variations only along single direction while in the other direction signal changes are relatively slow meaning that parameters can be estimated along single line (1-D signal) and summed or interpolated along the other. Here, we consider cases when signal phase is fast changing in both directions so it is important to consider estimation of parameters from 2-D signal and not from 1-D signal lines. Only two estimators (2-D CPF and 2-D (P)HAF-CPF) are considered, while similar generalization can be performed for all other estimators described in Section III.

A. 2-D CPF

Consider the following 2-D CP model:

$$y(n, m) = x(n, m) + \nu(n, m), \quad (89)$$

$$(n, m) \in [-N/2, N/2) \times [-M/2, M/2),$$

where

$$x(n, m) = Ae^{j\phi(n, m)} = Ae^{j\sum_{p=0}^3 \sum_{q=0}^{3-p} a_{p,q} n^p m^q}, \quad (90)$$

and $N \times M$ is size of the signal, $\nu(n, m)$ is a white complex Gaussian noise with zero-mean and variance σ^2 , i.e., $E\{\nu(n, m)\} = 0$ and $E\{\nu(n, m)\nu^*(n_1, m_1)\} = \sigma^2\delta(n - n_1, m - m_1)$. $\phi(n, m)$ is a polynomial phase with total order up to 3, and $a_{p,q}$ is the $(p+q)$ -layer parameter. The 2-D model in (90) is called the 2-D triangular form (see [72], [74], [76], [77]). The signal support region is $N \times M$.

By introducing the auto-correlation of the following form

$$r_{yy}(n, m; \tau_n, \tau_m) = y(n + \tau_n, m + \tau_m)y(n - \tau_n, m - \tau_m), \quad (91)$$

the 2-D CPF is defined as

$$C(n, m; \Psi) = \sum_{\tau_n} \sum_{\tau_m} r_{yy}(n, m; \tau_n, \tau_m) e^{-j\psi_n \tau_n^2 - j\psi_m \tau_m^2} \times e^{-j2\psi_{nm} \tau_n \tau_m} \quad (92)$$

where $\Psi = (\psi_n, \psi_{nm}, \psi_m)$. For noise-free signal, the 2-D CPF is concentrated on the position of the partial derivatives of the signal phase $\psi_n = \partial^2 \phi(n, m) / \partial n^2$, $\psi_{nm} = \partial^2 \phi(n, m) / \partial n \partial m$, and $\psi_m = \partial^2 \phi(n, m) / \partial m^2$. These phase derivatives are related to the phase parameters as:

$$\begin{bmatrix} \frac{\partial^2 \phi(n, m)}{\partial n^2} \\ \frac{\partial^2 \phi(n, m)}{\partial n \partial m} \\ \frac{\partial^2 \phi(n, m)}{\partial m^2} \end{bmatrix} = \begin{bmatrix} 2a_{2,0} + 2a_{2,1}m + 6a_{3,0}n \\ a_{1,1} + 2a_{2,1}n + 2a_{1,2}m \\ 2a_{0,2} + 2a_{1,2}n + 6a_{0,3}m \end{bmatrix}. \quad (93)$$

Partial second-order derivatives can be estimated by calculating $C(n, m; \Psi)$ at three instants (n_1, m_1) , (n_2, m_2) , and (n_3, m_3) , by performing three 3-D searches:

$$\begin{aligned} \hat{\Omega}(n_i, m_i) &= [\hat{\Omega}_n(n_i, m_i), \hat{\Omega}_{nm}(n_i, m_i), \hat{\Omega}_m(n_i, m_i)] \\ &= \arg \max_{\Psi} |C(n_i, m_i; \Psi)|, \quad i = 1, 2, 3. \end{aligned} \quad (94)$$

Then, seven phase parameters including the four third-layer ones and the three second-layer ones $\{\hat{a}_{p+q} | p+q = 3 \vee p+q = 2\}$ are estimated as:

$$\begin{aligned} \begin{bmatrix} \hat{a}_{2,0} \\ \hat{a}_{3,0} \\ \hat{a}_{2,1} \end{bmatrix} &= \begin{bmatrix} 2 & 6n_1 & 2m_1 \\ 2 & 6n_2 & 2m_2 \\ 2 & 6n_3 & 2m_3 \end{bmatrix}^{-1} \begin{bmatrix} \hat{\Omega}_n(n_1, m_1) \\ \hat{\Omega}_n(n_2, m_2) \\ \hat{\Omega}_n(n_3, m_3) \end{bmatrix}, \\ \begin{bmatrix} \hat{a}_{0,2} \\ \hat{a}_{0,3} \\ \hat{a}_{1,2} \end{bmatrix} &= \begin{bmatrix} 2 & 6m_1 & 2n_1 \\ 2 & 6m_2 & 2n_2 \\ 2 & 6m_3 & 2n_3 \end{bmatrix}^{-1} \begin{bmatrix} \hat{\Omega}_m(n_1, m_1) \\ \hat{\Omega}_m(n_2, m_2) \\ \hat{\Omega}_m(n_3, m_3) \end{bmatrix}, \\ \begin{bmatrix} \hat{a}_{1,1} \\ \hat{a}_{2,1} \\ \hat{a}_{1,2} \end{bmatrix} &= \begin{bmatrix} 1 & 2n_1 & 2m_1 \\ 1 & 2n_2 & 2m_2 \\ 1 & 2n_3 & 2m_3 \end{bmatrix}^{-1} \begin{bmatrix} \hat{\Omega}_{nm}(n_1, m_1) \\ \hat{\Omega}_{nm}(n_2, m_2) \\ \hat{\Omega}_{nm}(n_3, m_3) \end{bmatrix}. \end{aligned} \quad (95)$$

The lower-layer phase parameters and the amplitude can be estimated in a straightforward manner as in [93]. Note that the dechirping technique is used again to estimate the zero-layer phase parameter $a_{0,0}$, the first-layer phase parameters $a_{0,1}$ and $a_{1,0}$, and the amplitude. Therefore, these estimates undergo the error-propagation effects from the third-layer and second-layer parameter estimation. Nevertheless, the second-layer parameter estimation is free of the error-propagation effects, while the 2-D HAF [72], [76], [77], approach introduces the error propagation to the second-layer parameter estimates.

Since the 2-D CPF results in a 3-D function of $[\psi_n, \psi_{nm}, \psi_m]$ for a fixed instant pair (n, m) , a 3-D search is required to locate the maxima in the 2-D CPF (94). Instead of the 3-D search, the GA or other meta-heuristic techniques can be employed. For details on the implementation of the GA refer to [67].

The 2-D CPF is an unbiased estimator, i.e., $E\{\hat{a}_{i,j}\} = a_{i,j}$ for the second and third-layer coefficients $i+j \geq 2$. For the second-layer phase parameters, the estimator is asymptotically efficient, i.e., the variance of parameter estimate for high SNR approaches to the CRLB, while for the third-order layers it

MSE is slightly above the CRLB (less than 1.7dB above for all coefficients):

$$\begin{aligned} E\{(\delta a_{2,0})^2\} &= \left(1 + \frac{1}{2\text{SNR}}\right) \left[\frac{90}{\text{SNR} N^5 M}\right] \\ &= \left(1 + \frac{1}{2\text{SNR}}\right) \text{CRLB}\{a_{2,0}\}, \end{aligned} \quad (96)$$

$$\begin{aligned} E\{(\delta a_{0,2})^2\} &= \left(1 + \frac{1}{2\text{SNR}}\right) \left[\frac{90}{\text{SNR} M^5 N}\right] \\ &= \left(1 + \frac{1}{2\text{SNR}}\right) \text{CRLB}\{a_{0,2}\}, \end{aligned} \quad (97)$$

$$\begin{aligned} E\{(\delta a_{1,1})^2\} &= \left(1 + \frac{1}{2\text{SNR}}\right) \left[\frac{72}{\text{SNR} M^3 N^3}\right] \\ &= \left(1 + \frac{1}{2\text{SNR}}\right) \text{CRLB}\{a_{1,1}\}, \end{aligned} \quad (98)$$

$$\begin{aligned} E\{(\delta a_{3,0})^2\} &= \left(1.4543 + \frac{1.3175}{\text{SNR}}\right) \left[\frac{1400}{\text{SNR} N^7 M}\right] \\ &= \left(1.4543 + \frac{1.3175}{\text{SNR}}\right) \text{CRLB}\{a_{3,0}\}, \end{aligned} \quad (99)$$

$$\begin{aligned} E\{(\delta a_{0,3})^2\} &= \left(1.4543 + \frac{1.3175}{\text{SNR}}\right) \left[\frac{1400}{\text{SNR} N M^7}\right] \\ &= \left(1.4543 + \frac{1.3175}{\text{SNR}}\right) \text{CRLB}\{a_{0,3}\}, \end{aligned} \quad (100)$$

$$\begin{aligned} E\{(\delta a_{2,1})^2\} &= \left(\frac{4}{3} + \frac{2}{\text{SNR}}\right) \left[\frac{1080}{\text{SNR} N^5 M^3}\right] \\ &= \left(\frac{4}{3} + \frac{2}{\text{SNR}}\right) \text{CRLB}\{a_{2,1}\}, \end{aligned} \quad (101)$$

$$\begin{aligned} E\{(\delta a_{1,2})^2\} &= \left(\frac{4}{3} + \frac{2}{\text{SNR}}\right) \left[\frac{1080}{\text{SNR} N^3 M^5}\right] \\ &= \left(\frac{4}{3} + \frac{2}{\text{SNR}}\right) \text{CRLB}\{a_{1,2}\}. \end{aligned} \quad (102)$$

For high SNR, the term with $1/\text{SNR}^2$ may be negligible.

B. 2-D HAF-CPF

Similar to the 1-D signals, the 2-D CPF is limited to the third-order 2-D-PPSs. Therefore, combination with the 2-D HAF (frequently called Francos-Friedlander (FF) approach) is desirable in order to reduce the signal to 2-D CP that can be further processed by the 2-D CPF. This technique is studied in [101] and compared with relevant counterparts showing significant improvement in the accuracy (both MSE is reduced and SNR threshold) [67], [194]- [196].

Results obtained with the 2-D (P)HAF-CPF are better than 2-D (P)HAF counterparts since number of PDs is reduced with respect to the latter case. However, it could require search over 3-D space that could be demanding and meta-heuristic search techniques for complexity reduction.

C. Numerical examples

Example 6. Performance of the 2-D CPF-based approach is compared with the FF-based technique on the third-order 2-D PPS with parameters: $A = 1$, $a_{0,0} = 1$, $a_{1,0} = 4.5 \cdot 10^{-1}$, $a_{0,1} = 6.2 \cdot 10^{-2}$, $a_{2,0} = -1.5 \cdot 10^{-3}$, $a_{1,1} = -3 \cdot 10^{-3}$, $a_{0,2} = -2.2 \cdot 10^{-3}$, $a_{3,0} = 2.7 \cdot 10^{-5}$, $a_{2,1} = 4 \cdot$

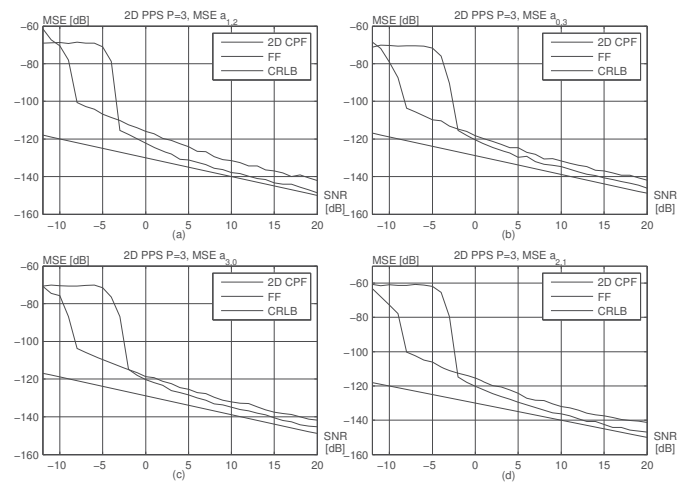


Fig. 6. MSEs of the highest-layer phase parameters obtained by the 2-D CPF and FF for the third-order 2-D PPS: (a) MSEs of parameter $a_{1,2}$; (b) MSEs of parameter $a_{0,3}$; (c) MSEs of parameter $a_{3,0}$ and (d) MSEs of parameter $a_{2,1}$.

10^{-5} , $a_{1,2} = 3.73 \cdot 10^{-5}$, $a_{0,3} = -1.35 \cdot 10^{-5}$ and $N = M = 100$. The considered SNR range is $\text{SNR} \in [-12, 20]$ dB. Search optimization in the 2-D CPF is performed using the GA with setup proposed in [101], while parameters in the FF algorithm are chosen following instructions from [76]. MSEs of the highest layer phase parameters are shown in Figure 6 and are obtained using Monte Carlo simulations with 200 trials. As it can be seen from Figure 6, the SNR threshold of the 2-D CPF is at -8 dB, while the FF-based approach has the SNR threshold at -2 dB. The FF-based approach for $\text{SNR} > -2$ dB has from 3 dB to 5 dB lower MSE with respect to the 2-D CPF. Larger MSE of the 2D CPF is influenced by the GA used for the search optimization.

Example 7. In this example, performances for both the 2-D HAF-CPF and FF-based approaches are evaluated. Considered signal is the fourth-order 2-D PPS with following parameters: $A = 1$, $a_{0,0} = 1$, $a_{1,0} = 4.5 \cdot 10^{-1}$, $a_{0,1} = 8.2 \cdot 10^{-2}$, $a_{2,0} = -1.5 \cdot 10^{-3}$, $a_{1,1} = 6 \cdot 10^{-3}$, $a_{0,2} = -2.2 \cdot 10^{-3}$, $a_{3,0} = 1.7 \cdot 10^{-5}$, $a_{2,1} = 4 \cdot 10^{-5}$, $a_{1,2} = 3.73 \cdot 10^{-5}$, $a_{0,3} = -1.35 \cdot 10^{-5}$, $a_{0,4} = 4.5 \cdot 10^{-6}$, $a_{4,0} = -2.3 \cdot 10^{-6}$, $a_{1,3} = 1.23 \cdot 10^{-6}$, $a_{3,1} = 3.2 \cdot 10^{-6}$, $a_{2,2} = 6.2 \cdot 10^{-6}$ and $N = M = 100$. Again, the GA setup from [101] is used for the search optimization in the 2-D HAF-CPF. Experiments are performed using Monte Carlo simulations with 200 trials. MSEs of four characteristic phase parameters of the highest-layer are shown of Figure 7. Similar results as for the third-order 2-D PPS are obtained here. The 2-D HAF-CPF has for 4dB lower SNR threshold than the FF-based approach. However, due to error influenced by the stochastic search strategies, it has from 3dB to 5dB larger MSE. Note that the accuracy of the 2-D HAF-CPF can be improved up to the CRLB using parameter refinement strategy proposed in [270].

V. APPLICATIONS

In the following, we provide a brief literature overview with applications of the CPF and its variants. The most important application appears to be radar signal processing given in

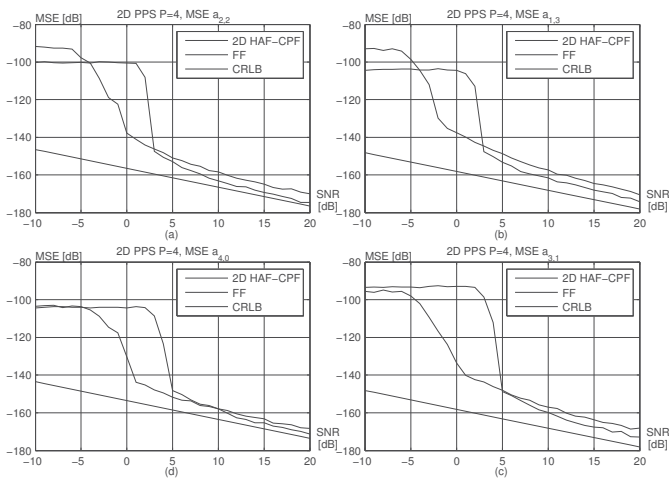


Fig. 7. MSEs of the highest-layer phase parameters obtained by the 2-D HAF-CPF and FF for the fourth-order 2-D PPS: (a) MSEs of parameter $a_{2,2}$; (b) MSEs of parameter $a_{1,3}$; (c) MSEs of parameter $a_{4,0}$, and (d) MSEs of parameter $a_{3,1}$.

Section V-A, while application to joint estimation of the signal parameters and direction (angle)-of-arrival (DOA) to sensor array systems is presented in Section V-B. Section V-C summarizes other fields where the PPS appears to be a valid signal model.

A. CPF in radar signal processing

As already stated, the most important application of the CPF and related techniques with huge number of papers is in the radar signal processing. The reason is in the fact that the radar returns can be modeled as multicomponent PPSs at the output of the matched filter. Some details on the principles of the radar systems can be found in [197]- [200] with modeling of radar returns in [201].

The SAR and ISAR images are in general 2-D FT of received returns. In the case when returns are 2-D sinusoids obtained images are ideal, i.e., sharp. However, due to radar or target motion and other effects obtained signal could be distorted to form of sum of 2-D PPSs. In order to get sharper image it is required to demodulate received signals in order to compensate polynomial modulation. The CPF is excellent tool for such applications since often received signal can be modeled as a sum of 2-D CP signals [98], [99]. Sometimes polynomial modulation of all targets or scatterers is the same and PPS parameters can be estimated at once. However, in the case when modulation of received signals is different alternative strategies are employed like, for example, considering each received signal separately, or estimation of signal parameters for each line of radar image, or estimation of parameters of the strongest signal followed by consecutive estimation weaker signals [65], [66]. When signal parameters are estimated, signal is dechirped in order to obtain sharp radar images. In some applications, sharp radar image is not goal of the processing but important information related to targets or their parts can be extracted from the received PPS parameters [237].

The CPF and related transforms are applied to almost all kinds of the radar systems including synthetic aperture radar systems (SAR), inverse synthetic aperture radar systems (ISAR), and over-the-horizon radar systems (OTHR) where the CPF and related tools are applied or where CP signals appear. Some of these papers are summarized below.

It seems that over the half of the paper where the PPS estimation is considered in the field of modern radar systems is in the ISAR where due to target motion or extreme target maneuvering the radar returns contain one or more PPS components possibly with high-order phase terms [65], [161], [202]- [218]. Fast maneuvering targets are addressed in [219]- [225] while issues associated with slowly moving targets are addressed in [226]. Numerous emerging research papers are concentrated to the shipborne ISAR systems and challenging problem of vessels monitoring with similar tools or models have been considered in [227]- [232]

SAR systems [61], [233], are also attracting recently attention of the research community [66], [98], [99], [175], [234]- [236].

Micro-Doppler effect caused by rotating and vibrating parts of the targets is addressed in [162], [237], while the Doppler shift is considered in [238], [239].

The OTHR systems [240] produce rather challenging signatures with multiple close components in the TF plane in addition to other undesired effects such as clutter and fast amplitude variations. Problem of clutter is addressed in [241], while passive acoustics radars are presented in [95]. Radar systems able to precisely monitor multi-aircraft formation are considered in [242]. Modulation pulse compression radars are analyzed in [239].

B. CPF in DOA estimation

One of important fields where the PPSs appear are sensor array networks. In this case, in addition to the signal parameter estimation it is important to estimate parameters related to geometry of the network and source position and/or motion. Consider the simplest geometry of the sensor array called the uniform linear array (ULA). In order to improve the estimation of the PPS parameters it is important to utilize as much information related to signals from all sensors.

Assume a constant amplitude PPS $x(t)$ impinging on an ULA with M omnidirectional sensors. The output can be written as [243]

$$\mathbf{y}(t) = \mathbf{a}(\theta, t)x(t) + \mathbf{v}(t), \quad |t| \leq (N-1)/2, \quad (103)$$

where $\mathbf{a}(\theta, t)$ is the $M \times 1$ array steering vector, $\mathbf{v}(n)$ the $M \times 1$ vector of i.i.d. complex Gaussian zero-mean noise samples, and N the number of samples. The P th order PPS $x(t)$ is defined as

$$x(t) = Ae^{j\phi(t)} = Ae^{j\sum_{k=0}^P a_k t^k}, \quad (104)$$

where A is the amplitude, $\phi(t)$ the phase with coefficients $a_k, k = 0, \dots, K$. The steering vector $\mathbf{a}(\theta, t)$ can be modelled

as in [78]

$$\begin{aligned} \mathbf{a}(\boldsymbol{\theta}, t) &= [1, e^{j\omega(t)\psi}, \dots, e^{j\omega(t)(M-1)\psi}]^T, \\ \omega(t) &= \frac{d\phi(t)}{dt} = \sum_{k=0}^{K-1} (k+1)a_{k+1}t^k, \\ \psi &= d \frac{\sin(\theta)}{c}, \end{aligned} \quad (105)$$

where $\omega(t)$ is the IF of the PPS, θ is the DOA, d is the inter-sensor spacing, and c the propagation speed. The goal is the joint estimation of the vector $\mathbf{V} = [\theta, a_1, \dots, a_K]$ from observations $\mathbf{y}(t)$.

Note that this signal model is simplification under assumption that the term $\omega(t)(M-1)\psi$ is relatively small [78]. However, in the case when it is not satisfied then more general and difficult model can arise where received signal on the l th sensor can be modeled as

$$y_l(t) = A e^{j\phi(t-l\psi)} = A e^{j \sum_{k=0}^P a_k (t-l\psi)^k}. \quad (106)$$

In both cases the fact that the CPF and related techniques give possibility to estimate parameters with smaller number of PDs is important. More details on joint PPS and DOA estimation can be found in [8], [9], [78], [243]- [246].

C. Other applications

The CPF-based PPS parameter estimator can also be applied to the underwater acoustics [247]. However, processing of the underwater acoustic narrowband signals may be more challenging than the radar signal processing.

The PPS signals appear in optics and more recently in holographic interferometry [248]- [251], and coherent laser remote sensing [252]. Another interesting area is power networks where the PPS appears in transient process [253], [254].

The PPSs appear in diverse contexts in the electronic warfare [255], [256], including jammer excision [257]. A lot of attention has also been paid to research related to the medical [2], [100], [258]- [260], and biological signals [261]. Finally, it is worthy mentioning recent advances in communications [262], and statistical mechanics [107].

VI. CONCLUSION

This paper has reviewed recent progresses in the PPS parameter estimation and in related fields motivated and inspired by the CPF. In less than 15 years, the CPF has attracted significant attention and numerous upgrades that improve significantly standard PD-based techniques in the PPS estimation. One of the aim of this paper is to demonstrate that such a simple modification has ability to advance a research field and to clear the major obstacles of the state-of-the-art methods.

It should be admitted that in addition to the CPF there are some other parallel developments in the field of the PPS estimation. For example, O'Shea has proposed refinement strategy [263] that is able to reduce MSE in the PPS estimation to the CRLB for the SNR above the SNR threshold. There are quite important developments related to the phase unwrapping estimators [28]. Next, important development is the quasi ML approach that is reducing search space in the PPS estimation with accuracy close to the ML estimators [26]. It seems that

all these developments were possible only when O'Shea with the CPF had shown that there is still significant room for improvements in the PPS estimation.

We have mentioned several issues that are currently not well understood and where in particular theoretical development can shed new lights to the CPF. One of such issues is systematic handling the multicomponent signals and geometry of auto- and cross-terms [125]. The second issue is potential for generalization of the CPF like the WD in the TF analysis is generalized to the Cohen class of distribution [151], [176]. Also, it is important to investigate if it is possible to establish relationship between CPF and the FrFT in similar manner as the STFT is generalized to the high-order TF representations [145], [148], [151]. Another issue is to investigate if sharpening techniques can be applied to the CPF in the time-CR domain like reassignment approach in the TF analysis [136]- [141]. Similarly, investigation of the synchrosqueezing [264], [265], S-transform, and other time-scale methods to the CR estimation problem could be of importance [266]- [269]. These issues do not limit potential theoretical developments in the area of joint time-CR domain representations. Improvement achieved with the CPF and related approaches will surely bring more advanced applications.

REFERENCES

- [1] B. Boashash, "Estimating and interpreting the instantaneous frequency of a signal. Part I: Fundamentals," *Proc. IEEE*, Vol. 80, No. 4, pp. 521-538, Apr. 1992.
- [2] —, "Estimating and interpreting the instantaneous frequency of a signal. Part II: Algorithms and applications," *Proc. IEEE*, Vol. 80, No. 4, pp. 540-568, Apr. 1992.
- [3] B. Barkat, "Instantaneous frequency estimation of nonlinear frequency-modulated signals in the presence of multiplicative and additive noise," *IEEE Trans. Sig. Proc.*, Vol. 49, No.10, pp. 2214-2222, Oct. 2001.
- [4] P. Flandrin, *Time-frequency/time-scale analysis*, Academic Press, 1999.
- [5] P. O'Shea, R. A. Wiltshire, "A new class of multilinear functions for polynomial phase signal analysis," *IEEE Trans. Signal Processing*, Vol. 57, No. 6, pp. 2096-2109, June 2009.
- [6] P. O'Shea, "Improving polynomial phase parameter estimation by using nonuniformly spaced signal sample methods," *IEEE Trans. Signal Processing*, Vol. 60, No. 7, pp. 3405-3414, July 2012.
- [7] S. Peleg, B. Porat, "Estimation and classification of polynomial-phase signals," *IEEE Trans. Inf. Th.*, Vol. 37, pp. 422-430, Mar. 1991.
- [8] A. Amar, "Efficient estimation of a narrow-band polynomial phase signal impinging on a sensor array," *IEEE Trans. Signal Processing*, Vol. 58, pp. 923-927, Feb. 2010.
- [9] A. Amar, A. Leshem, A. J. van der Veen, "A low complexity blind estimator of narrowband polynomial phase signals," *IEEE Trans. Signal Processing*, Vol. 58, pp. 4674-4683, Sep. 2010.
- [10] R. Kumaresan, S. Verma, "On estimating the parameters of chirp signals using rank reduction techniques," in *Proc. Asilomar Conf Signals. Syst. Comput.*, pp. 555-558, 1987.
- [11] S. Golden, B. Friedlander, "A modification of the discrete polynomial transform," *IEEE Trans. Sig. Proc.*, Vol. 46, pp. 1452-1455, May 1998.
- [12] B. Porat, B. Friedlander, "Accuracy analysis of estimation algorithms for parameters of multiple polynomial-phase signals," in *Proc. IEEE ICASSP*, pp. 1800-1803, May 1995.
- [13] B. Friedlander, "Parametric signal analysis using the polynomial phase transform," in *Proc. IEEE WHOS*, pp. 151-159, June 1993.
- [14] P. O'Shea, "Fast parameter estimation algorithms for linear FM signals," in *Proc. IEEE ICASSP*, Vol. 4, pp. 17-20, Apr. 1994.
- [15] S. Peleg, B. Porat, B. Friedlander, "The achievable accuracy in estimating the instantaneous phase and frequency of a constant amplitude signal," *IEEE Trans. Signal Processing*, Vol. 43, pp. 2216-2224, June 1995.
- [16] A. Scaglione, S. Barbarossa, "Statistical analysis of the product high-order ambiguity function," *IEEE Trans. Inform. Theory*, Vol. 45, pp. 343-356, Jan. 1999.

- [17] A. M. Zoubir, D. R. Iskander, "Bootstrap modeling of a class of nonstationary signals," *IEEE Trans. Sig. Proc.*, Vol. 48, pp. 399–408, Feb. 2000.
- [18] S. Djukanović, I. Djurović, "Aliasing detection and resolving in the estimation of polynomial-phase signal parameters," *Signal Processing*, Vol. 92, 235–239, 2012.
- [19] I. Djurović, M. Simeunović, B. Lutovac, "Are genetic algorithms useful for the parameter estimation of FM signals?," *Digital Signal Processing*, Vol. 22, pp. 1137–1144, 2012.
- [20] B. Porat, B. Friedlander, "Blind deconvolution of polynomial-phase signals using the high-order ambiguity function," *Signal Processing*, Vol. 53, pp. 149–163, 1996.
- [21] A. Swami, "Polyphase signals in additive and multiplicative noise: CRLB and HOS," in *Proc. Sixth IEEE Signal Processing Workshop DSP*, pp. 109–112, Oct. 1994.
- [22] M. Z. Ikram, G. T. Zhou, "Estimation of multicomponent polynomial phase signals of mixed orders," *Sig. Proc.*, Vol. 81, pp. 2293–2308, 2001.
- [23] Y. Wang Y, G. T. Zhou, "On the use of high-order ambiguity function for multi-component polynomial phase signals," *Sig. Proc.*, Vol. 65, pp. 283–296, 1998.
- [24] A. Ferrari, C. Theys, G. Alengrin, "Polynomial-phase signal analysis using stationary moments," *Sig. Proc.*, Vol. 54, pp. 239–248, 1996.
- [25] I. Djurović, L.J. Stanković, "STFT-based estimator of polynomial phase signals," *Sig. Proc.*, Vol. 92, No. 11, pp. 2769–2774, Nov. 2012.
- [26] —, "Quasi maximum likelihood estimator of polynomial phase signals," *IET Sig. Proc.*, Vol. 13, No. 4, pp. 347–359, 2014.
- [27] G. T. Zhou, Y. Wang, "Exploring lag diversity in the high-order ambiguity function for polynomial phase signals," *IEEE Signal Process. Lett.*, Vol. 4, pp. 240–242, Aug. 1997.
- [28] R. G. McKilliam, B. G. Quinn, I. V. L. Clarkson, B. Moran, B. N. Vellambi, "Polynomial phase estimation by least squares phase unwrapping," *IEEE Trans. Signal Process.*, Vol. 62, pp. 1962–1975, Apr. 2014.
- [29] S. Shamsunder, G. B. Giannakis, B. Friedlander, "Estimating random amplitude polynomial phase signals: A cyclostationary approach," *IEEE Trans. Signal Processing*, Vol. 43, pp. 492–505, Feb. 1995.
- [30] G. T. Zhou, G. B. Giannakis, A. Swami, "On polynomial phase signals with time-varying amplitudes," *IEEE Trans. Signal Processing*, Vol. 44, pp. 848–861, Apr. 1996.
- [31] S. Shamsunder, G. Giannakis, "Detection and estimation of chirp signals in non-Gaussian noise," in *Proc of Asilomar Conf. Signals, Syst. Comput.*, pp. 1191–1195, Nov. 1993.
- [32] G. T. Zhou, A. Swami, "Performance analysis for a class of amplitude modulated polynomial phase signals," in *Proc. of IEEE ICASSP*, pp. 1593–1596, 1995.
- [33] M. R. Morelande, A. M. Zoubir, "On the performance of cyclic moments-based parameter estimators of amplitude modulated polynomial phase signals," *IEEE Trans. Signal Processing*, Vol. 50, pp. 590–606, Mar. 2002.
- [34] M. Ghogho, A. K. Nandi, A. Swami, "Cramér–Rao bound and maximum likelihood estimation for random amplitude phase modulated signals," *IEEE Trans. Signal Processing*, Vol. 47, pp. 2905–2916, Nov. 1999.
- [35] B. Friedlander, J. Francos, "Estimation of amplitude and phase of nonstationary signals," in *Proc. of Asilomar Conf. Signals, Syst. Comput.*, pp. 431–435, Nov. 1993.
- [36] M. Jabloun, N. Martin, F. Leonard, M. Vieira, "Estimation of the instantaneous amplitude and frequency of non-stationary short-time signals," *Signal Processing*, Vol. 88, pp. 1636–1655, 2008.
- [37] A. T. Johansson, P. R. White, "Instantaneous frequency estimation at low signal-to-noise ratios using time-varying notch filters," *Signal Processing*, Vol. 88, pp. 1271–1288, 2008.
- [38] C. Theys, A. Ferrari, M. Vieira, "Marginal Bayesian analysis of polynomial-phase signals," *Signal Processing*, Vol. 81, pp. 69–82, 2001.
- [39] S. Barbarossa, "Detection and estimation of the instantaneous frequency of polynomial phase signals by multilinear time-frequency representations," in *Proc. IEEE-SP Workshop Higher Order Stat.*, pp. 168–172, June 1993.
- [40] —, "Parameter estimation of multicomponent polynomial-phase signals by intersection of signal subspaces," in *Proc. IEEE-SP Workshop Stat. Signal Array Processing*, pp. 452–455, June 1996.
- [41] S. Barbarossa, R. Marneli, A. Scaglione, "Adaptive detection of polynomial-phase signals embedded in noise using high order ambiguity functions," in *Proc. of Asilomar Conf. Signals, Syst. Comput.*, Nov. 1997.
- [42] S. Barbarossa, A. Porchia, A. Scaglione, "Multiplicative multilag higher-order ambiguity function," in *Proc. of IEEE ICASSP*, Vol. 5, pp. 3022–3026, May 1996.
- [43] Y. Wang, G. T. Zhou, "On the use of high order ambiguity function for multicomponent polynomial phase signals," in *Proc. IEEE ICASSP*, Vol. 5, pp. 3629–3632, Apr. 1997.
- [44] P. Tichavsky, P. Handel, "Multicomponent polynomial phase signal analysis using a tracking algorithm," *IEEE Trans. Signal Processing*, Vol. 47, pp. 1390–1395, May 1999.
- [45] S. Tretter, "Estimating the frequency of a noisy sinusoid by linear regression," *IEEE Trans. Inf. Th.*, Vol. 31, pp. 832–835, Nov. 1985.
- [46] H. Fu, P. Y. Kam, "MAP/ML estimation of the frequency and phase of a single sinusoid in noise," *IEEE Trans. Signal Processing*, Vol. 55, No. 3, pp. 834–845, Mar. 2007.
- [47] Y. Li, H. Fu, P. Y. Kam, "Improved, approximate, time-domain ML estimators of chirp signal parameters and their performance analysis," *IEEE Trans. Signal Process.*, Vol. 57, pp. 1260–1272, Apr. 2009.
- [48] R. G. McKilliam, I. V. L. Clarkson, "Identifiability and aliasing in polynomial-phase signals," *IEEE Trans. Sig. Proc.*, Vol. 57, pp. 4554–4557, 2009.
- [49] H. L. V. Trees, *Detection, estimation and modulation theory*, Wiley, 1968.
- [50] Z. M. Deng, L. M. Ye, M. Z. Fu, S. J. Lin, Y. X. Zhang, "Further investigation on time-domain maximum likelihood estimation of chirp signal parameters," *IET Signal Process.*, Vol. 7, pp. 444–449, July 2013.
- [51] X. Lv, G. Bi, C. Wang, M. Xing, "Lv's distribution: principle, implementation, properties, and performance," *IEEE Trans. Signal Process.*, Vol. 59, No. 8, pp. 3576–3591, 2011.
- [52] S. Luo, G. Bi, X. Lv, F. Hu, "Performance analysis on Lv distribution and its applications," *Dig. Sig. Proc.*, Vol. 23, No. 3, pp. 797–807, 2013.
- [53] X. Guo, H. Sun, S. Wang, G. Liu, "Comments on 'discrete chirp-Fourier transform and its application to chirp rate estimation'," *IEEE Trans. Signal Process.*, Vol. 50, No. 12, p. 3115, 2012.
- [54] X. G. Xia, "Discrete chirp-Fourier transform and its application to chirp rate estimation," *IEEE Trans. Signal Process.*, Vol. 48, No. 11, pp. 3122–3133, 2000.
- [55] M. R. Morelande, "Parameter estimation of phase-modulated signals using Bayesian unwrapping," *IEEE Transactions on Signal Processing*, Vol. 57, No. 11, pp. 4209–4219, 2009.
- [56] S. Ma, J. Jiang, Q. Meng, "A fast, accurate and robust method for joint estimation of frequency and frequency rate," in *Proc. of ISPACS*, pp. 1–6, 2011.
- [57] Y. Yang, Z. Peng, X. Dong, W. Zhang, G. Meng, "Application of parameterized time-frequency analysis on multicomponent frequency modulated signals," *IEEE Transactions on Instrumentation and Measurement*, Vol. 63, No. 12, pp. 3169–3180, 2014.
- [58] B. Boashash, *Time frequency signal analysis and processing: a comprehensive reference*. Boston: Elsevier, 2003.
- [59] —, *Time frequency signal analysis and processing: a comprehensive reference*, Second edition, Amsterdam: Academic Press, Elsevier, 2016.
- [60] L. Cirillo, A. Zoubir, M. Amin, "Parameter estimation for locally linear FM signals using a time-frequency Hough transform," *IEEE Trans. Sig. Proc.*, Vol. 56, No. 9, pp. 4162–4175, Sep. 2008.
- [61] J. C. Curlander, R. N. McDonough, *Synthetic Aperture Radar - System and Signal Processing*, John Wiley & Sons, New York, 1991.
- [62] P. M. Djurić, S. Kay, "Parameter estimation of chirp signals," *IEEE Trans. Sig. Proc.*, Vol. 38, No. 12, pp. 2118–2126, Dec. 1990.
- [63] I. Djurović, L.J. Stanković, "Realization of the robust filters in the frequency domain," *IEEE Sig. Proc. Lett.*, Vol. 9, No. 10, pp. 333–335, Oct. 2002.
- [64] —, "Modification of the ICI rule based IF estimator for high noise environments," *IEEE Trans. Sig. Proc.*, Vol. 52, No. 9, pp. 2655–2661, 2004.
- [65] I. Djurović, T. Thayaparan, L.J. Stanković, "Adaptive local polynomial Fourier transform in ISAR," *Journal of Applied Signal Processing*, Vol. 2006, Article ID 36093, 2006.
- [66] —, "SAR imaging of moving targets using polynomial FT," *IET Proc. Sig. Proc.*, Vol. 2, No. 3, pp. 237–246, 2008.
- [67] I. Djurović, P. Wang, C. Ioana, "Parameter estimation of 2-D cubic phase signal using cubic phase function with genetic algorithm," *Sig. Proc.*, Vol. 90, No. 9, pp. 2698–2707, Sep. 2010.
- [68] D. L. Donoho, P. J. Huber, The notion of breakdown point, in *E.L. Lehmann Festschrift*, P. J. Bickel, K. Doksum, and J. L. Hodges, Jr., Eds. Belmont, CA: Wadsworth.
- [69] M. Farquharson, P. O'Shea, "Extending the performance of the cubic phase function algorithm," *IEEE Tran. Sig. Proc.*, Vol. 55, No. 10, Oct. 2007.

- [70] M. Farquharson, P. O'Shea, G. Ledwich, "A computationally efficient technique for estimating the parameters of polynomial phase signals from noisy observations," *IEEE Tran. Sig. Proc.*, Vol. 53, No. 8, pp. 3337-3342, Aug. 2005.
- [71] M. Fliess, M. Mboup, H. Mounier, H. Sira-Ramirez, "Questioning some paradigms of signal processing via concrete examples," *Algebraic Methods in Flatness, Signal Processing and State Estimation*, pp. 1-21, 2003.
- [72] J. M. Francos, B. Friedlander, "Two-dimensional polynomial phase signals: parameter estimation and bounds," *Multidim. Syst. and Sig. Proc.*, Vol. 9, No. 2, pp. 173-205, Apr. 1998.
- [73] —, "Optimal parameter selection in the phase differencing algorithm for 2-D phase estimation," *IEEE Trans. Signal Proc.*, Vol. 47, No. 1, pp. 273-279, Jan. 1999.
- [74] —, "Parameter estimation of 2-D random amplitude polynomial-phase signals," *IEEE Trans. Signal Proc.*, Vol. 47, No. 7, pp. 1795-1810, July 1999.
- [75] B. Friedlander, J. M. Francos, "Estimation of amplitude and phase parameters of multicomponent signals," *IEEE Trans. Sig. Proc.*, Vol. 43, No. 4, pp. 917-926, Apr. 1995.
- [76] —, "An estimation algorithm for 2-D polynomial phase signals," *IEEE Trans. Im. Proc.*, Vol. 5, No. 6, pp. 1084-1087, 1996.
- [77] B. Friedlander, J. M. Francos, "Model based phase unwrapping of 2-D signals," *IEEE Trans. Sig. Proc.*, Vol. 44, No. 12, pp. 2999-3007, 1996.
- [78] A. B. Gershman, M. Pesavento, M. G. Amin, "Estimating parameters of multiple wideband polynomial-phase sources in sensor arrays," *IEEE Trans. Signal Proc.*, Vol. 49, No.12, pp. 2924-2934, Dec. 2001.
- [79] D. E. Goldberg, *Genetic algorithms in search, optimization, and machine learning*, Addison-Wesley.
- [80] Z. M. Hussain, B. Boashash, "Adaptive instantaneous frequency estimation of multicomponent FM signals using quadratic time-frequency distributions," *IEEE Trans. Signal Proc.*, Vol. 50, pp. 1676-1866, Aug. 2002.
- [81] V. Katkovnik, K. Egiazarian, J. Astola, "Application of the ICI principle to window size adaptive median filtering," *Sig. Proc.*, Vol. 83, No. 1, pp. 251-257, Feb. 2003.
- [82] V. Katkovnik, L.J. Stanković, "Instantaneous frequency estimation using the Wigner distribution with varying and data driven window length," *IEEE Trans. Sig. Proc.*, Vol. 46, No. 9, pp. 2315-2325, Sep. 1998.
- [83] V. Katkovnik, L.J. Stanković, "Periodogram with varying and data-driven window length," *Sig. Proc.*, Vol. 67, No. 3, pp. 345-358, 1998.
- [84] B. Krstajić, L.J. Stanković, Z. Uskoković, "An approach to variable step-size LMS algorithm," *El. Lett.*, Vol. 38, No. 16, pp. 927-928, Aug. 2002.
- [85] I. Mann, S. McLaughlin, W. Henkel, R. Kirby, T. Kessler, "Impulse generation with appropriate amplitude, length, and spectral characteristics," *IEEE Journal on Selected Areas in Communications*, Vol. 20, No. 5, pp. 901-912, June 2001.
- [86] D. Middleton, "Statistical-physical models of urban radio-noise environments - Part I: Fundamentals," *IEEE Trans. on Electromagnetic Compatibility*, Vol. 14, No. 2, pp. 38-56, May 1972.
- [87] C. L. Nikias, M. Shao, *Signal processing with alpha-stable distributions and applications*, John Wiley & Sons, 1995.
- [88] P. O'Shea, "A new technique for instantaneous frequency rate estimation," *IEEE Sig. Proc. Lett.*, Vol. 9, No. 8, pp. 252-252, Aug. 2002.
- [89] —, "A fast algorithm for estimating the parameters of a quadratic FM signal," *IEEE Trans. Sig. Proc.*, Vol. 52, No. 2, pp. 385-393, Feb. 2004.
- [90] S. Peleg, B. Friedlander, "The discrete polynomial phase transform," *IEEE Trans. Sig. Proc.*, Vol. 43, No. 8, pp. 1901-1914, Aug. 1995.
- [91] S. Peleg, B. Porat, "Linear FM signal parameter estimation from discrete-time observations," *IEEE Trans. Aerosp. Electron. Syst.*, Vol. 27, No. 4, pp. 607-614, July 1991.
- [92] S. Peleg, B. Friedlander, "Multicomponent signals analysis using the polynomial-phase transform," *IEEE Trans. Aerosp. Electron. Syst.*, Vol. 32, No. 1, pp. 378-387, Jan. 1996.
- [93] B. Porat, *Digital processing of random signals: Theory and methods*. Englewood Cliffs, NJ: Prentice-Hall, 1994.
- [94] B. Porat, B. Friedlander, "Asymptotic statistical analysis of the high-order ambiguity function for parameter estimation of polynomial-phase signals," *IEEE Trans. Inform. Theory*, Vol. 42, No. 3, pp. 995-1001, May 1996.
- [95] D. C. Reid, A. M. Zoubir, B. Boashash, "Aircraft flight parameter estimation based on passive acoustic techniques using the polynomial Wigner-Ville distribution," *J. Acoust. Soc. Amer.*, Vol. 102, No. 1, pp. 207-223, July 1997.
- [96] S. Barbarossa, A. Scaglione, G. B. Giannakis, "Product high-order ambiguity function for multicomponent polynomial-phase signal modeling," *IEEE Trans. Sig. Proc.*, Vol. 46, No. 3, pp. 691-708, Mar. 1998.
- [97] S. Barbarossa, V. Petrone, "Analysis of polynomial-phase signals by the integrated generalized ambiguity function," *IEEE Trans. Sig. Proc.*, Vol. 45, No. 2, pp. 316-327, Feb. 1997.
- [98] J. J. Sharma, C. H. Gierull, M. J. Collins, "The influence of target acceleration on velocity estimation in dual-channel SAR-GMTI," *IEEE Trans. Geoscience and Remote Sensing*, Vol. 44, No. 1, pp. 134-147, Jan. 2006.
- [99] —, "Compensating the effects of target acceleration in dual-channel SARCGMTI," *IEE Proc. Radar Sonar Navigation*, Vol. 153, No. 1, pp. 53-62, Feb. 2006.
- [100] Y. Pantazis, O. Rosec, Y. Stylianou, "Chirp rate estimation of speech based on a time-varying quasi-harmonic model," in *Proc. of IEEE ICASSP*, pp. 3985-3988, 2009.
- [101] I. Djurović, M. Simeunović, S. Djukanović, P. Wang, "A hybrid CPF-HAF estimation of polynomial-phase signals: detailed statistical analysis," *IEEE Transactions on Signal Processing*, Vol. 60, No. 10, pp. 5010-5023, Oct. 2012.
- [102] M. Simeunović, I. Djurović, "CPF-HAF estimator of polynomial-phase signals," *El. Lett.*, Vol. 47, No. 17, pp. 965-966, Aug. 2011.
- [103] I. Djurović, M. Simeunović, "Combined HO-CPF and HO-WD PPS estimator," *Sig. Im. Vid. Proc.*, Vol. 9, No. 6, pp. 1395-1400, Sep. 2015.
- [104] M. Simeunović, I. Djurović, "Non-uniform sampled cubic phase function," *Signal Processing*, Vol. 101, pp. 99-103, Aug. 2014.
- [105] I. Djurović, M. Simeunović, "Parameter estimation of non-uniform sampled polynomial-phase signals using the HOCPP-WD," *Signal Processing*, Vol. 106, No. 1, pp. 253-258, Jan. 2015.
- [106] T. H. Cormen, C. E. Leiserson, R. L. Rivest, C. Stein, *Introduction to algorithms*, 3rd Edition, The MIT Press, July 2009.
- [107] N. Merhav, "Threshold effects in parameter estimation as phase transitions in statistical mechanics," *IEEE Transactions on Information Theory*, Vol. 57, No. 10, pp. 7000-7010, Oct. 2011.
- [108] B. Ristić, B. Boashash, "Comments on 'The Cramer-Rao lower bounds for signals with constant amplitude and polynomial phase'," *IEEE Transactions on Signal Processing*, Vol. 46, No. 6, pp. 1708-1709, June 1998.
- [109] S. Peleg, B. Porat, "The Cramer-Rao lower bound for signals with constant amplitude and polynomial phase," *IEEE Transactions on Signal Processing*, Vol. 39, No. 3, pp. 749-752, March 1991.
- [110] J. A. Legg, D. A. Gray, "Performance bounds for polynomial phase parameter estimation with non-uniform and random sampling schemes," *IEEE Transactions on Signal Processing*, Vol. 48, No. 2, pp. 331-337, Feb. 2000.
- [111] J. Angeby, "Aliasing of polynomial-phase signal parameters," *IEEE Trans. Sig. Proc.*, Vol. 48, No. 5, pp. 1488-1491, May 2000.
- [112] L.J. Stanković, I. Djurović, S. Stanković, M. Simeunović, M. Daković, "Instantaneous frequency in time-frequency analysis: Enhanced concepts and performance of estimation algorithms," *Digital Signal Processing*, Vol. 35, pp. 1-13, Dec. 2014.
- [113] M. Jabloun, F. Leonard, M. Vieira, N. Martin, "A new flexible approach to estimate the IA and IF of nonstationary signals of long-time duration," *IEEE Transactions on Signal Processing*, Vol. 55, No. 7, pp. 3633-3644, 2007.
- [114] L.J. Stanković, "Multitime definition of the Wigner higher order distribution: L-Wigner distribution," *IEEE Signal Processing Letters*, Vol. 1, No. 7, pp. 106-109, July 1994.
- [115] L.J. Stanković, S. Stanković, "An analysis of instantaneous frequency presentation using time-frequency distributions - Generalized Wigner distribution," *IEEE Transactions on Signal Processing*, Vol. 43, No. 2, pp. 549-552, Feb. 1995.
- [116] L.J. Stanković, "A time-frequency distribution concentrated along the instantaneous frequency," *IEEE Sig. Proc. Lett.*, Vol. 3, No. 3, pp. 89-91, Mar. 1996.
- [117] T. Abotzoglou, "Fast maximum likelihood joint estimation of frequency and frequency rate," *IEEE Trans. on Aerosp. Electron. Syst.*, Vol. 22, pp. 708-715, Nov. 1986.
- [118] N. Nguyen, Q. H. Liu, "The regular Fourier matrices and nonuniform fast Fourier transforms," *SIAM J. Sci. Comput.*, Vol. 21, No. 1, pp. 283-293, 1999.
- [119] Q. H. Liu, N. Nguyen, X. Y. Tang, "Accurate algorithms for nonuniform fast forward and inverse Fourier transforms and their applications," in *Proc. of IEEE Geosci. Remote Sensing Symp.*, Vol. 1, pp. 288-290, 1998.

- [120] I. Djurović, C. Ioana, L.J. Stanković, P. Wang, "Adaptive algorithm for chirp-rate estimation," *EURASIP Journal on Advances in Signal Processing*, Vol. 2009, Article ID 727034, 9 pages, doi:10.1155/2009/727034.
- [121] L.J. Stanković, "Adaptive instantaneous frequency estimation using TFDs," in *Time-frequency signal analysis and processing*, B. Boashash, Ed. New York: Elsevier, 2003.
- [122] —, "Performance analysis of the adaptive algorithm for bias-to-variance tradeoff," *IEEE Trans. Sig. Proc.*, Vol. 52, No. 5, pp. 1228-1234, May 2004.
- [123] L.J. Stanković, V. Katkovnik, "Algorithm for the instantaneous frequency estimation using time-frequency distributions with variable window width," *IEEE Signal Processing Lett.*, Vol. 5, pp. 224-228, Sept. 1998.
- [124] —, "Instantaneous frequency estimation using higher order distributions with adaptive order and window length," *IEEE Trans. Inform. Theory*, Vol. 46, pp. 302-311, Jan. 2000.
- [125] F. Hlawatsch, G. F. Boudreaux-Bartels, "Linear and quadratic time-frequency signal representations," *IEEE Signal Processing Magazine*, Vol. 9, No. 2, pp. 21-67, Apr. 1992.
- [126] B. Ristić, B. Boashash, "Kernel design for time-frequency analysis using Radon transform," *IEEE Transactions on Signal Processing*, Vol. 41, No. 5, pp. 1996-2008, May 1993.
- [127] J. C. Wood, D. T. Barry, "Radon transform of time-frequency distributions for analysis of multicomponent signals," *IEEE Transactions on Signal Processing*, Vol. 42, No. 1, pp. 3166-3177, Nov. 1994.
- [128] S. Barbarossa, O. Lemoine, "Analysis of nonlinear FM signals by pattern recognition of their time-frequency representation," *IEEE Signal Processing Letters*, Vol. 3, No. 4, pp. 112-115, Apr. 1996.
- [129] M. Wang, A. K. Chan, C. K. Chui, "Linear frequency-modulated signal detection using Radon-ambiguity transform," *IEEE Trans. Signal Process.*, Vol. 46, No. 3, pp. 571-586, 1998.
- [130] L. Cohen, *Time-frequency analysis*, Prentice-Hall, New York, 1995.
- [131] —, "Time-frequency distributions - A review," *Proceedings of the IEEE*, Vol. 77, No. 7, pp. 941-981, 1989.
- [132] B. Barkat, B. Boashash, "Design of higher order polynomial Wigner-Ville distributions," *IEEE Tran. Sig. Proc.*, Vol. 47, No. 9, pp. 2608-2610, Sep. 1999.
- [133] S. Stanković, L.J. Stanković, "An approach to the polynomial Wigner-Ville distributions," in *Proc. IEEE TFTA*, June 1996, pp.153-156.
- [134] L.J. Stanković, "Time-frequency distributions with complex argument," *IEEE Trans. Sig. Proc.*, Vol. 50, No. 3, March 2002, pp. 475-486.
- [135] S. Stanković, L.J. Stanković, "Introducing time-frequency distribution with a "complex-time" argument," *Electronics Letters*, Vol. 32, No. 14, July 1996, pp. 1265-1267.
- [136] F. Auger, P. Flandrin, "Improving the readability of time-frequency and time-scale representations by reassignment method," *IEEE Trans. Signal Process.*, Vol. 43, May 1995, pp. 1068-1089.
- [137] E. Chassande-Mottin, I. Daubechies, F. Auger, P. Flandrin, "Differential reassignment," *IEEE Signal Proc. Lett.*, Vol. 4, No. 10, pp. 293-294, Oct. 1997.
- [138] S. Barbarossa, "Analysis of multicomponent LFM signals by a combined Wigner-Hough transform," *IEEE Trans. Sig. Proc.*, Vol. 43, No. 6, pp. 1511-1515, Jun. 1995.
- [139] P. Wang, J. Yang, "Parameter estimation of multicomponent quadratic FM signals using computationally efficient Radon-CPF transform," in *Proc. of IEEE Signal Processing Conference*, pp. 1-5, 2006.
- [140] C. Richard, R. Lengelle, "Joint recursive implementation of time-frequency representations and their modified version by the reassignment method," *Signal Processing*, Vol. 60, No. 2, pp. 163-179, 1997.
- [141] I. Djurović, L.J. Stanković, "Time-frequency representation based on the reassigned S-method," *Sig. Proc.*, Vol. 77, No. 1, pp. 115-120, Aug. 1999.
- [142] D. L. Jones, R. G. Baraniuk, "An adaptive optimal-kernel time-frequency representations," *IEEE Transactions on Signal Processing*, Vol. 43, No. 10, pp. 2361-2371, Oct. 1995.
- [143] N. A. Khan, B. Boashash, "Multi-component instantaneous frequency estimation using locally adaptive directional time frequency distributions," *Int. J. Adapt. Control Signal Process.*, 2016, Vol. 30, pp. 429-442.
- [144] L. Zuo, M. Li, Z. Liu, L. Ma, "A high-resolution time-frequency rate representation and the cross-term suppression," *IEEE Transactions on Signal Processing*, Vol. 64, No. 10, pp. 2463-2474, May. 2016.
- [145] L. B. Almeida, "The fractional Fourier transform and time-frequency representations," *IEEE Trans. Sig. Proc.*, Vol. 42, No. 11, pp. 3084-3091, Nov. 1994.
- [146] A. Bultheel, H. Martnez-Sulbaran, "Recent developments in the theory of the fractional Fourier and linear canonical transforms," *The Bulletin of the Belgian Mathematical Society - Simon Stevin*, Vol. 13, No. 5, pp. 971-1005, Jan. 2007.
- [147] L.J. Stanković, T. Alieva, M. J. Bastiaans, "Time-frequency signal analysis based on the windowed fractional Fourier transform," *Signal Processing*, Vol. 83, No. 11, pp. 2459-2468, Nov. 2003.
- [148] E. Sejdić, I. Djurović, L.J. Stanković, "Fractional Fourier transform as a signal processing tool: An overview of recent developments," *Special issue on the Fourier related transforms, Signal Processing*, Vol. 91, No. 6, pp. 1351-1369, June 2011.
- [149] X. Li, G. Bi, S. Stankovic, A. M. Zoubir, "Local polynomial Fourier transform: A review on recent development and applications," *Signal Process.*, Vol. 90, No. 6, pp. 1370-1393, 2011.
- [150] R. G. Dorsch, A. W. Lohmann, Y. Bitran, D. Mendlovic, "Chirp filtering in the fractional Fourier domain," *Appl. Opt.*, Vol. 33, pp. 7599-7602, 1994.
- [151] L.J. Stanković, "Quadratic and higher order time-frequency analysis based on the STFT," in *Time-Frequency Signal Analysis and Processing*, ed. B. Boashash, Academic Press, Dec. 2015.
- [152] M. R. Portnoff, "Time-frequency representation of digital signals and systems based on short-time Fourier analysis," *IEEE Trans. Acoust. Speech. Signal Process.*, Vol. 28, No. 1, pp. 55-69, 1980.
- [153] P. Wang, I. Djurović, J. Yang, "Modifications of the cubic phase function," *Chin. Jour. of Electr.*, Vol.17, No.1, pp. 189-194, Jan. 2008.
- [154] —, "Generalized high-order phase function for parameter estimation of polynomial phase signal," *IEEE Trans. on Signal Processing*, Vol. 56, No. 7, pp. 3023-3028, July 2008.
- [155] P. Wang, P. V. Orlik, K. Sadamoto, W. Tsujita, and F. Gini, "Parameter estimation of hybrid sinusoidal FM-polynomial phase signal," *IEEE Signal Processing Letters*, in print.
- [156] M. Z. Ikram, K. Abed-Meraim, Y. Hua, "Fast quadratic phase transform for estimating the parameters of multicomponent chirp signals," *Digital Signal Processing*, Vol. 7, pp. 127-135, 1997.
- [157] G. Bi, Y. Wei, G. Li, C. Wang, "Radix-2 DIF fast algorithms for polynomial time-frequency transforms," *IEEE Transactions on Aerosp. Electron. Syst.*, Vol. 42, No. 4, pp. 1540-1546, 2006.
- [158] Y. Ju, G. Bi, "Generalized fast algorithms for the polynomial time frequency transforms," *IEEE Transactions on Signal Processing*, Vol. 55, No. 10, pp. 4907-4915, Oct. 2007.
- [159] G. Bi, Y. Ju, X. Li, "Fast algorithms for polynomial time-frequency transforms of real-valued sequences," *IEEE Transactions on Signal Processing*, Vol. 56, No. 5, pp. 1905-1915, May 2008.
- [160] P. Wang, H. Li, I. Djurović, B. Himes, "Integrated cubic phase function for linear FM signal analysis," *IEEE Trans. on Aerospace and Electronic Systems*, Vol. 46, No. 3, pp. 963-977, July 2010.
- [161] J. Zheng, T. Su, L. Zhang, W. Zhu, Q. H. Liu, "ISAR imaging of targets with complex motion based on the chirp rate-quadratic chirp rate distribution," *IEEE Transactions on Geoscience and Remote Sensing*, Vol. 52, No. 11, pp. 7276-7289, 2014.
- [162] P. Li, D.-C. Wang, and J.-L. Chen, "Parameter estimation for micro-Doppler signals based on cubic phase function," *Signal, Image and Video Processing*, Vol. 7, No. 6, 2013, pp. 1239-1249.
- [163] G. Bi, X. Li, C. M. See, "LFM signal detection using LPP-Hough transform," *Signal Processing*, Vol. 91, No. 6, pp. 1432-1443, 2011.
- [164] X. Lv, M. Xing, S. Zhang, Z. Bao, "Keystone transformation of the Wigner-Ville distribution for analysis of multicomponent LFM signals," *Signal Process.*, Vol. 89, No. 5, pp. 791-806, 2009.
- [165] P. Wang, J. Yang, I. Djurović, "Algorithm extension of cubic phase function for estimating quadratic FM signal," in *Proc. of IEEE ICASSP*, Vol. 3, pp. 1125-1128, 2007.
- [166] L.J. Stanković, "Local polynomial Wigner distributions," *Signal Processing*, Vol. 59, No. 1, pp. 123-128, May 1997.
- [167] P. Wang, I. Djurović, J. Yang, "Instantaneous frequency rate estimation based on robust cubic phase function," in *Proc. of IEEE ICASSP'06*, Sept. 2006.
- [168] I. Djurović, V. V. Lukin, "Robust DFT with high breakdown point for complex-valued impulse noise environment," *IEEE Signal Processing Letters*, Vol. 13, No. 1, pp. 25-28, Jan. 2006.
- [169] V. Katkovnik, I. Djurović, L.J. Stanković, "Robust time-frequency distributions," in *"Time-frequency signal analysis and applications"*, Academic press, 2nd edition, editor B. Boashash pp. 539-546, Dec. 2015.
- [170] M. Simeunović, S. Djukanović, I. Djurović, "A fine search method for the cubic-phase function-based estimator," *EUSIPCO 2012*, pp. 924-928, Aug. 2012.

- [171] S. Djukanović, M. Simeunović, I. Djurović, "Estimation refinement techniques for the cubic phase function," in *Proc. of Telfor*, pp. 727-730, 2011.
- [172] E. Aboutanios, B. Mulgrew, "Iterative frequency estimation by interpolation on Fourier coefficients," *IEEE Transactions on Signal Processing*, Vol. 53, No. 4, pp. 1237-1242, Apr. 2005.
- [173] E. Aboutanios, "Estimating the parameters of sinusoids and decaying sinusoids in noise," *IEEE Instrumentation & Measurement Magazine*, Vol. 14, No. 2, pp. 8-14, Apr. 2011.
- [174] I. Djurović, S. Djukanović, V. V. Lukin, "An algorithm for the fine estimation of polynomial-phase signals," *IEEE Transactions on Aerospace and Electronics Systems*, Vol. 48, No. 4, pp. 3687-3693, Oct. 2012.
- [175] I. Djurović, C. Ioana, T. Thayaparan, L.J. Stanković, P. Wang, V. Popović, M. Simeunović, "Cubic phase function evaluation for multicomponent signals with application to SAR imaging," *IET Signal Processing*, Vol. 4, No. 4, pp. 371-381, Aug. 2010.
- [176] L.J. Stanković, "A method for time-frequency signal analysis," *IEEE Trans. Sig. Proc.*, Vol. 42, No. 1, pp. 225-229, Jan. 1994.
- [177] N. Otsu, "A threshold selection method from gray-level histograms," *IEEE Trans. Sys., Man, Cyber.*, Vol. 9, No. 1, pp. 62-66, 1979.
- [178] I. Djurović, S. Djukanović, M. G. Amin, Y. D. Zhang, and B. Himed, "High-resolution time-frequency representations based on the local polynomial Fourier transform for over-the-horizon radars," *Radar Sensor Technology XVI*, edited by Kenneth I. Ranney, Armin W. Doerry, Proc. of SPIE Vol. 8361, doi: 10.1117/12.919954.
- [179] I. Djurović, V. V. Lukin, M. Simeunović, B. Barkat, "Quasi maximum likelihood estimator of polynomial phase signals for compressed sensed data," *AEUE International Journal of Electronics and Communications*, Vol. 68, No. 7, pp. 631-636, July 2014.
- [180] L.J. Stanković, M. Daković, "On the uniqueness of the sparse signals reconstruction based on the missing samples variation analysis," *Mathematical Problems in Engineering*, Vol. 2015, Article ID 629759, 14 pages, 2015. doi:10.1155/2015/629759.
- [181] S. Stanković, L.J. Stanković, I. Orović, "Compressive sensing approach in the Hermite transform domain," *Mathematical Problems in Engineering*, Vol. 2015, Article ID 286590, 9 pages <http://dx.doi.org/10.1155/2015/286590>.
- [182] S. Stanković, I. Orović, L.J. Stanković, "An automated signal reconstruction method based on analysis of compressive sensed signals in noisy environment," *Signal Processing*, Vol. 104, pp. 43 - 50, Nov. 2014.
- [183] D. L. Donoho, "For most large underdetermined systems of linear equations the minimal ℓ_1 -norm solution is also the sparsest solution," *Communications on pure and applied mathematics*, Vol. 59, No. 6, pp. 797-829, 2006.
- [184] —, "Compressed sensing," *IEEE Transactions on Information Theory*, Vol. 52, No. 4, pp. 1289-1306, Apr. 2006.
- [185] E. J. Candes, J. K. Romberg, T. Tao, "Stable signal recovery from incomplete and inaccurate measurements," *Communications on pure and applied mathematics*, Vol. 59, No. 8, pp. 1207-1223, 2006.
- [186] —, "Robust uncertainty principles: exact signal reconstruction from highly incomplete frequency information," *IEEE Transactions on Information Theory*, Vol. 52, No. 2, pp. 489-509, Feb. 2006.
- [187] B. Jokanović, M. Amin, and T. Dogaru, "Time-frequency signal representations using interpolations in joint-variable domains," *IEEE Geoscience and Remote Sensing Letters*, Vol. 12, No. 1, pp. 204-208, Jan. 2015.
- [188] S. Ghofrani, M. G. Amin, Y. D. Zhang, "High-resolution direction finding of non-stationary signals using matching pursuit," *Signal Processing*, Vol. 93, No. 12, pp. 3466-3478, Dec. 2013.
- [189] I. Djurović, "Viterbi algorithm for chirp-rate and instantaneous frequency estimation," *Sig. Proc.*, Vol. 91, No. 5, pp. 1308-1314, May 2011.
- [190] A. J. Viterbi, "Error bounds for convolutional codes and an asymptotically optimum decoding algorithm," *IEEE Transactions on Information Theory*, Vol. 13, No. 2, pp. 260-269, Apr. 1967.
- [191] G. D. Forney, "The Viterbi algorithm," *Proceedings of the IEEE*, Vol. 61, No. 3, pp. 268-278, Mar. 1973.
- [192] I. Djurović, L.J. Stanković, "An algorithm for the Wigner distribution based instantaneous frequency estimation in a high noise environment," *Signal Processing*, Vol. 84, No. 3, pp. 631-643, Mar. 2004.
- [193] C. Cornu, I. Djurović, C. Ioana, A. Quinquis, L.J. Stanković, "Time-frequency detection using Gabor filter banks and Viterbi based grouping algorithm," in *Proc. of IEEE ICASSP'2005*, Vol. 4, pp.497-500, Mar. 2005.
- [194] M. Simeunović, I. Djurović, "Parameter estimation of multicomponent 2D polynomial-phase signals using the 2D PHAF-based approach," *IEEE Transactions on Signal Processing*, Vol. 64, No. 3, pp. 771-782, Feb. 2016.
- [195] S. Barbarossa, P. Di Lorenzo, P. Vecchiarelli, "Parameter estimation of 2-D multi-component polynomial phase signals: An application to SAR imaging of moving targets," *IEEE Transactions on Signal Processing*, Vol. 62, No. 17, pp. 4375-4389, Sep. 2014.
- [196] I. Djurović, "Quasi ML algorithm for 2-D PPS estimation," *Multidimensional Signals and Systems*, in print.
- [197] N. Levanov, *Radar principles*, Wiley-Interscience, New York, 1988.
- [198] D. R. Wehner, *High-resolution radar*, Artech House, Norwood, MA, 1995.
- [199] A. W. Rihaczek, *Principles of high-resolution radar*, McGraw-Hill, New York, 1969.
- [200] J. B. Tsui, *Digital techniques for wideband receivers*, Raleigh: Scitech, 2004.
- [201] R. P. Perry, R. C. Dipietro, R. L. Fante, "SAR imaging of moving targets," *IEEE Trans. Aer. El. Syst.*, Vol. 35, No. 1, pp. 188-200, 1999.
- [202] Y. Wang, "Inverse synthetic aperture radar imaging of manoeuvring target based on range-instantaneous-Doppler and range-instantaneous-chirp-rate algorithms," *IET Radar, Sonar & Navigation*, Vol. 6, No. 9, pp. 921-928, 2012.
- [203] M. Xing, R. Wu, Y. Li, Z. Bao, "New ISAR imaging algorithm based on modified Wigner-Ville distribution," *IET Radar, Sonar and Navigation*, Vol.3, No. 1, pp. 70-80, 2008.
- [204] X. Lv, M. Xing, C. Wang, S. Zhang, "ISAR imaging of maneuvering targets based on the range centroid Doppler technique," *IEEE Trans. Image Process.*, Vol. 19, No. 1, pp. 141-153, 2010.
- [205] Y. Wang, Y. Jiang, "Inverse synthetic aperture radar imaging of maneuvering target based on the product generalized cubic phase function," *IEEE Geosci. Remote Sens. Lett.*, Vol. 8, No. 5, pp. 958-962, 2011.
- [206] Y. Wang, Y. Lin, "ISAR imaging of non-uniformly rotating target via range-instantaneous-Doppler-derivatives algorithm," *IEEE J. Sel. Top. Appl. Ear. Obs. Rem. Sens.*, Vol. 7, No. 1, pp. 167-176, 2014.
- [207] Y. Wang, J. Kang, Y. Jiang, "ISAR imaging of maneuvering target based on the local polynomial Wigner distribution and integrated high-order ambiguity function for cubic phase signal model," *IEEE J. Sel. Top. Appl. Ear. Obs. Rem. Sens.*, Vol. 7, No. 7, pp. 2971-2991, 2014.
- [208] Y. Wang, B. Zhao, J. Kang, "Asymptotic statistical performance of local polynomial Wigner distribution for parameters estimation of ship target," *IEEE J. Sel. Top. Appl. Earth Obs. Rem Sens.*, Vol. 8, No. 3, pp. 1087-1098, 2015.
- [209] L. Wu, X. Wei, D. Yang, H. Wang, X. Li, "ISAR imaging of targets with complex motion based on discrete chirp Fourier transform for cubic chirps," *IEEE Trans. Geosci. Remote Sens.*, Vol. 50, No. 10, pp. 4201-4212, Oct. 2012.
- [210] Y. Li, T. Su, J. Zheng, X. He, "ISAR imaging of targets with complex motions based on modified Lv's distribution for cubic phase signal," *IEEE J. Sel. Topics Appl. Earth Observ. Remote Sens.*, Vol. 8, No. 10, pp. 4775-4784, 2015.
- [211] J. Zheng, T. Su, W. Zhu, L. Zhang, Z. Liu, Q. H. Liu, "ISAR imaging of nonuniformly rotating target based on a fast parameter estimation algorithm of cubic phase signal," *IEEE Trans. Geosci. Remote Sens.*, Vol. 53, No. 9, pp. 4727-4740, 2015.
- [212] J. Xu, X. G. Xia, S. B. Peng, J. Yu, Y. N. Peng, L. C. Qian, "Radar maneuvering target motion estimation based on generalized Radon-Fourier transform," *IEEE Transactions on Signal Processing*, Vol. 60, No. 12, pp. 6190-6201, 2012.
- [213] J. Wang, D. Kasilingam, "Global range alignment for ISAR," *IEEE Trans. Aer. Elec. Syst.*, Vol. 39, No. 1, pp. 351-357, 2003.
- [214] K. Wang, L. Luo, Z. Bao, "Global optimum method for alignment in ISAR imagery," in *Proc. of Radar*, pp. 14-16, 1997.
- [215] D. Zhu, L. Wang, Y. Yu, Q. Tao, Z. Zhu "Robust ISAR range alignment via minimizing the entropy of the average range profile," *IEEE Geosci. Remote Sens. Let.*, Vol. 6, No. 2, pp. 204-208, 2009.
- [216] J. Zheng, H. Liu, G. Liao, T. Su, Z. Liu, Q.-H. Liu, "ISAR imaging of targets with complex motions based on a noise-resistant parameter estimation algorithm without nonuniform axis," *IEEE Sensors Journal*, Vol. 16, No. 8, pp. 2509-2518, 2015.
- [217] X. Li, G. Liu, J. Ni, "Autofocusing of ISAR imaging based on entropy minimization," *IEEE Trans. AES*, Vol. 35, No. 4, pp. 1240-1251, 1999.
- [218] Q. Lv, T. Su, J. Zheng, "Inverse synthetic aperture radar imaging of targets with complex motion based on the local polynomial ambiguity function," *Journal of Applied Remote Sensing*, Vol. 10, No. 1, 2016, doi: 10.1117/1.JRS.10.015019.

- [219] G. Sun, M. Xing, X. Xia, Y. Wu, Z. Bao, "Robust ground moving-target imaging using deramp-keystone processing," *IEEE Trans. Geosci. Remote Sens.*, Vol. 51, No. 2, pp. 966-982, Oct. 2013.
- [220] X. Chen, J. Guan, N. Liu, Y. He, "Maneuvering target detection via radon-fractional Fourier transform-based long-time coherent integration," *IEEE Trans. Signal Process.*, Vol. 62, No. 4, pp. 939-953, 2014.
- [221] X. Li, G. Cui, W. Yi, L. Kong, "A fast maneuvering target motion parameters estimation algorithm based on ACCF," *IEEE Signal Processing Letters*, Vol. 22, No. 3, pp. 270-274, 2015.
- [222] X. Li, G. Cui, L. Kong, W. Yi, X. Yang, J. Wu, "High speed maneuvering target detection based on joint keystone transform and CP function," in *Proc of IEEE Radar*, 2014, pp. 436-440.
- [223] X. Li, L. Kong, G. Cui, W. Li, "A low complexity coherent integration method for maneuvering target detection," *Digital Signal Processing*, Vol. 49, pp. 137-147, 2016.
- [224] X. Chen, Y. Huang, N. Liu, J. Guan, Y. He, "Radon-fractional ambiguity function-based detection method of low-observable maneuvering target," *IEEE Transactions on Aerospace and Electronic Systems*, Vol. 51, No. 2, pp. 815-833, 2015.
- [225] J. Ma, H. Tao, P. Huang, "Subspace-based super-resolution algorithm for ground moving target imaging and motion parameter estimation," *IET Radar, Sonar & Navigation*, Vol. 10, No. 3, pp. 488-499, 2015.
- [226] L. Yanyan, T. Su, Z. Jibin, X. He, "Inverse synthetic aperture radar imaging of targets with nonsevere maneuverability based on the centroid frequency chirp rate distribution," *Journal of Applied Remote Sensing*, Vol. 9, No. 1, doi: 10.1117/1.JRS.9.095065, 2015.
- [227] Y. Wang, Y. Jiang, "ISAR imaging of a ship target using product high order matched-phase transform," *IEEE Geosci. Remote Sens. Lett.*, Vol. 6, No. 4, pp. 658-661, 2009.
- [228] X. Bai, R. Tao, Z. Wang, Y. Wang, "ISAR imaging of a ship target based on parameter estimation of multicomponent quadratic frequency-modulated signals," *IEEE Trans. Geosci. Remote Sens.*, Vol. 52, No. 2, pp. 1418-1429, Feb. 2014.
- [229] J. Zheng, T. Su, G. Liao, H. Liu, Z. Liu, Q. H. Liu, "ISAR imaging for fluctuating ships based on a fast bilinear parameter estimation algorithm," *IEEE J. Sel. Topics Appl. Earth Observ. Remote Sens.*, Vol. 8, No. 8, pp. 3954-3966, 2015.
- [230] Y. Wang, Y. Jiang, "New approach for ISAR imaging of ship target with 3D rotation," *Mult. Syst. Sig. Proc.*, Vol. 21, No. 4, pp. 301-318, 2010.
- [231] S. Sun, Y. Jiang, Y. Yuan, B. Hu, T.-S. Yeo, "Defocusing and distortion elimination for shipborne bistatic ISAR," *Remote Sensing Letters*, Vol. 7, No. 6, pp. 523-532, 2016.
- [232] Y. Li, K. Liu, R. Tao, X. Bai, "Adaptive Viterbi-based range-instantaneous Doppler algorithm for ISAR Imaging of ship target at sea," *IEEE Journal of Oceanic Engineering*, Vol. 40, No. 2, pp. 417-425, 2015.
- [233] D. E. Wahl, P. H. Eichel, D. C. Ghiglia, "Phase gradient autofocus—a robust tool for high resolution SAR phase correction," *IEEE Trans. Aerosp. Electron. Syst.*, Vol. 30, No. 3, pp. 827-835, 1994.
- [234] L. Xianhua, X. Jintao, H. Yulin, W. Junjie, Y. Jianyu, W. Pu, "SAR Doppler frequency rate estimation based on time-frequency rate distribution," in *Proc. of APSAR*, pp. 926-930, 2009.
- [235] W. Li, J. Yang, Y. Huang, J. Wu, "High order doppler parameter estimation of bistatic forward-looking SAR based on CPF-Radon transform," in *Proc. of Int. Signal Processing Conference*, pp. 2239-2241, 2010.
- [236] W. Li, J. Yang, Y. Huang, L. Kong, "Third-order Doppler parameter estimation of bistatic forward-looking SAR based on modified cubic phase function," *IEICE Transactions on Communications*, Vol. 95, No. 2, pp. 581-586, 2012.
- [237] H. Yildiz, "Parameter estimation of multicomponent micro-Doppler signals," PhD thesis, Middle East technical University, 2014.
- [238] J. Zheng, T. Su, Q. H. Liu, L. Zhang, W. Zhu, "Fast parameter estimation algorithm for cubic phase signal based on quantifying effects of Doppler frequency shift," *Progress In Electromagnetics Research*, Vol. 142, pp. 57-74, 2013.
- [239] R. Tao, N. Zhang, Y. Wang, "Analyzing and compensating effects of range and Doppler frequency migrations in linear frequency modulation pulse compression radar," *IET Radar, Sonar and Navigation*, Vol. 5, No. 1, pp. 12-22, Jan. 2011.
- [240] J. Yi, X. Wan, F. Cheng, Z. Gong, "Computationally efficient RF interference suppression method with closed-form maximum likelihood estimator for HF surface wave over-the-horizon radars," *IEEE Trans. on Geos. and Rem. Sens.*, Vol. 51, No. 4, pp. 2361-2372, 2013.
- [241] H.-T. Tran, R. Melino, S. Kodituwakku, "Detection of accelerating targets in clutter using a de-chirping technique," Res. Report. No. DSTO-RR-0399. Defence science and technology organisation, Australia, 2014.
- [242] S.-B. Peng, J. Xu, X.-G. Xia, F. Liu, T. Long, J. Yang, Y.-N. Peng, "Multi-aircraft formation identification for narrowband coherent radar in a long coherent integration time," *IEEE Transactions on Aerospace and Electronic Systems*, Vol. 51, No. 3, pp. 2121-2137, 2015.
- [243] I. Djurović, S. Djukanović, M. Simeunović, P. Raković, B. Barkat, "An efficient joint estimation of wideband polynomial-phase signal parameters and direction-of-arrival in sensor array," *Eurasip Journal on Advances in Signal Processing*, <http://asp.eurasipjournals.com/content/2012/1/43>, 10 pages, 2012.
- [244] M. Adjrad, A. Belouchrani, "Estimation of multicomponent polynomial-phase signals impinging on a multisensor array using state-space modeling," *IEEE Transactions on Signal Processing*, Vol. 44, No. 1, pp. 32-45, 2007.
- [245] P. Raković, M. Simeunović, I. Djurović, "On improvement of joint estimation of DOA and PPS coefficients impinging on ULA," *Signal Processing*, in print.
- [246] S. Djukanović, M. Simeunović, I. Djurović, "Efficient parameter estimation of polynomial-phase signals impinging on a sensor array," in *Prof. of MEKO*, pp. 116-119, June 2012.
- [247] L. Xu, Y. Yang, L. Yang, "Localization of underwater tone noise sources using instantaneous frequency rate estimate," in *Proc. of IEEE Oceans*, pp. 1-7, 2013.
- [248] S. S. Gorthi, G. Rajshkhar, P. Rastogi, "Strain estimation in digital holographic interferometry using piecewise polynomial phase approximation based method," *Optics express*, Vol. 18, No. 2, pp. 560-565, 2010.
- [249] R. Kulkarni, P. Rastogi, "Multiple phase estimation in digital holographic interferometry using product cubic phase function," *Optics and Lasers in Engineering*, Vol. 51, No. 10, pp. 1168-1172, 2013.
- [250] S. S. Gorthi, P. Rastogi, "Phase estimation in digital holographic interferometry using cubic-phase-function based method," *Journal of Modern Optics*, Vol. 57, No. 7, pp. 595-600, 2010.
- [251] S. S. Gorthi, "Spatial fringe analysis methods and their application to holographic interferometry and fringe projection techniques," PhD thesis, EPFL, 2010.
- [252] B. Zang, Q. Li, H.-B. Ji, Y. Tang, "Quadratic phase error compensation algorithm based on phase cancellation for ISAR," in *Proc. of SPIE 8905*, doi:10.1117/12.2033135, Sep. 2013.
- [253] M. Glickman, S.-C. Kam, Z. Hussain, "The use of digital phase locked loops for estimation of instantaneous frequency rate in distributed power networks," in *Proc. of AUPEC*, pp. 1-3, 2007.
- [254] R. A. Wiltshire, "Analysis of disturbances in large interconnected power systems," PhD Thesis, QUT, 2007.
- [255] F. Digne, C. Cornu, A. Baussard, A. Khenchaf, D. Jahan, "Use of short-term polynomial phase estimation for new electronic warfare systems," in *Proc. of IET International Conference on Radar Systems*, pp.1-6, 2012.
- [256] —, "Short-term polynomial phase estimation: Application to radar signal in an electronic warfare context," in *Proc. of EUSIPCO*, pp. 2133-2137, 2012.
- [257] S. Djukanović, M. Daković, T. Thayaparan, L.J. Stanković, "Method for nonstationary jammer suppression in noise radar systems," *IET Signal Processing*, Vol. 4, No. 3, pp. 305-313, June 2010.
- [258] J. M. O'Toole, B. G. Zapirain, I. M. Saiz, A. B. A. Chen, I. Y. Santamaría, "Estimating the time-varying periodicity of epileptiform discharges in the electroencephalogram," in *Proc. of ISSPA*, pp. 1229-1234, 2012.
- [259] E. Vayrynen, K. Noponen, A. Vipin, T. X. Yuan, H. Al-Nashash, J. Kortelainen, A. All, "Automatic parametrization of somatosensory evoked potentials with chirp modeling," *IEEE Trans. Neural. Syst. Rehabil. Eng.*, in print.
- [260] B. Boashash, N. Ali Khan, T. Ben-Jabeur, "Time-frequency features for pattern recognition using high-resolution TFDs: A tutorial review," *Digital Signal Processing*, Vol. 40, pp. 1-30, May 2015.
- [261] J. DiCecco, J. E. Gaudette, J. A. Simmons, "Multi-component separation and analysis of bat echolocation calls," *The Journal of the Acoustical Society of America*, Vol. 133, No. 1, pp. 538-546, 2013.
- [262] G. Shao, P. She, X. Ren, "Nonstationary interference suppression in DSSS system using time-frequency distribution and polynomial phase signal model," in *Proc. of WiCom*, pp. 1-4, 2009.
- [263] P. O'Shea, "On refining polynomial phase signal parameter estimates," *IEEE Tran. Aer. El. Syst.*, Vol. 46, No. 3, pp. 978-987, July 2010.
- [264] I. Daubachies, J. Lu, H. Wu, "Synchrosqueezed wavelet transform: An empirical mode decomposition-like tool," *Applied and Computational Harmonic Analysis*, Vol. 30, No. 2, pp. 243-261, 2011.

- [265] T. Oberlin, S. Meigen, P. Perrier, "Second-order synchrosqueezing transform of invertible reassignment: towards ideal time-frequency presentation," *IEEE Transactions on Signal Processing*, Vol. 63, No. 3, pp. 1335-1344, 2015.
- [266] R. G. Stockwell, L. Mansinha, "The localization of the complex spectrum: S-transform," *IEEE Transactions on Signal Processing*, Vol. 44, No. 4, pp. 998-1001, April 1996.
- [267] G. Livanos, N. Ranganathan, J. Jiang, "Hearth sound analysis using the S-transform," in *Proc. of Comp. in Card.*, pp. 587-590, 2000.
- [268] R. G. Stockwell, "A basis for efficient representation of the S-transform," *Dig. Sig. Proc.*, Vol. 17, No. 1, pp. 371-393, Jan. 2007.
- [269] I. Djurović, E. Sejdić, J. Jiang, "Frequency based window width optimization for S-transform," *AEU – International Journal of Electronics and Communications*, Vol. 62, No. 4, pp. 245-250, Apr. 2008.
- [270] M. Simeunović, I. Djurović, S. Djukanović, "A novel refinement technique for 2-D PPS parameter estimation," *Signal Processing*, Vol. 2014, No. 94, pp. 251-254.